

ORSO: ACCELERATING REWARD DESIGN VIA ONLINE REWARD SELECTION AND POLICY OPTIMIZATION

Chen Bo Calvin Zhang^{*†‡}, Zhang-Wei Hong[†], Aldo Pacchiano^{§¶}, Pulkit Agrawal[†]
 Improbable AI Lab, Massachusetts Institute of Technology[†] ETH Zurich[‡]
 Boston University[§] Braod Institute of MIT and Harvard[¶]

ABSTRACT

Reward shaping is a critical component in reinforcement learning (RL), particularly for complex tasks where sparse rewards can hinder learning. While shaping rewards have been introduced to provide additional guidance, selecting effective shaping functions remains challenging and computationally expensive. This paper introduces Online Reward Selection and Policy Optimization (ORSO), a novel approach that frames shaping reward selection as an online model selection problem. ORSO employs principled exploration strategies to automatically identify promising shaping reward functions without human intervention, balancing exploration and exploitation with provable regret guarantees. We demonstrate ORSO’s effectiveness across various continuous control tasks using the Isaac Gym simulator. Compared to traditional methods that fully evaluate each shaping reward function, ORSO significantly improves sample efficiency, reduces computational time, and consistently identifies high-quality reward functions that produce policies comparable to those generated by domain experts through hand-engineered rewards.

1 INTRODUCTION

Reward functions are crucial in reinforcement learning (RL; Sutton & Barto (2018)) as they guide the learning of successful policies. In many real-world scenarios, the ultimate objective involves maximizing long-term rewards that are not immediately available, making optimization challenging. To address this, practitioners often introduce shaping rewards (Margolis & Agrawal, 2022; Liu et al., 2024; Mahmood et al., 2018; Ng et al., 1999) – to provide additional guidance during training. Instead of directly maximizing the task rewards (R), it is therefore common for the RL algorithm to maximize an easier-to-optimize shaped reward function F in the hope of obtaining high performance as measured by task rewards, R . While shaping rewards contain helpful hints, maximizing them does not necessarily solve the task. For instance, an agent tasked with finding an exit (i.e., longer-term reward in the future) may be provided with shaping rewards to avoid obstacles. However, the task success ultimately depends on reaching the exit, not just avoiding obstacles. If poorly designed, the shaped rewards F can mislead the RL algorithm, causing the agent to focus on maximizing F while neglecting R (Chen et al., 2022; Agrawal, 2021), leading to training failure or suboptimal performance.

Designing effective shaping reward functions F that improve RL algorithm performance is challenging and time-consuming. It requires multiple iterations of training agents with different shaping rewards, evaluating their performance on the task reward R , and refining F accordingly. This process is inefficient due to the lengthy training runs and because the performance measured early in training may be misleading, making it challenging to quickly iterate over different shaping rewards.

To address this challenge, we propose treating the design of the shaping reward function as an exploration-exploitation problem and to solve it using provably efficient online decision-making algorithms similar to those in multi-armed bandits (Auer et al., 2002; Auer, 2002) and model selection (Agarwal et al., 2017; Pacchiano et al., 2020; Dann et al., 2024; Foster et al., 2019; Lee et al., 2021). Each shaping reward function acts as an arm or model, with the agent’s task reward R when trained

^{*}Correspondence to cbczhang@mit.edu.

with shaping reward F serving as the model’s utility. Our goal is to identify the best shaping reward function within a fixed time budget.

This approach presents unique challenges. Unlike standard multi-armed bandit settings with stationary reward distributions, the utility of a shaping reward function in our case is nonstationary. As the agent explores new parts of the state space during training, the reward distribution changes. Additionally, we must balance exploration and exploitation to efficiently allocate training time among different shaping rewards without committing too early to high-performing options or wasting time on low-performing ones.

We introduce *Online Reward Selection and Policy Optimization* (ORSO), an algorithm that efficiently selects the best shaping reward function from a set of candidate shaping reward functions to improve RL performance on the task reward. ORSO provides regret guarantees and adaptively allocates training time to each shaping reward based on a model selection algorithm at each step. Our empirical results across various continuous control tasks using the Isaac Gym simulator (Makoviychuk et al., 2021) demonstrate that ORSO identifies the best auxiliary reward function much faster ($2\times$ or more) than current methods. Moreover, ORSO consistently selects reward functions that are comparable to, and sometimes surpass, those designed by domain experts.

2 PRELIMINARIES

Reinforcement Learning (RL) In RL, the objective is to learn a policy for an agent (e.g., a robot) that maximizes the expected cumulative reward during the interaction with the environment. The interaction between the agent and the environment is formulated as a Markov decision process (MDP) (Puterman, 2014), $\mathcal{M} = (\mathcal{S}, \mathcal{A}, P, r, \gamma, \rho_0)$, where the \mathcal{S} and \mathcal{A} denote state and action spaces, respectively, $P : \mathcal{S} \times \mathcal{A} \rightarrow \Delta_{\mathcal{S}}^1$ is the state transition dynamics, $r : \mathcal{S} \times \mathcal{A} \rightarrow \Delta_{\mathbb{R}}$ denotes the reward function, $\gamma \in [0, 1)$ is the discount factor, and $\rho_0 \in \Delta_{\mathcal{S}}$ is the initial state distribution. At each timestep $t \in \mathbb{N}$ of interaction, the agent selects an action $a_t \sim \pi(\cdot | s_t)$ based on its policy π , receives a (possibly) stochastic reward $r_t \sim r(s_t, a_t)$, and transitions to the next state $s_{t+1} \sim P(\cdot | s_t, a_t)$ according to the transition dynamics. Here, r is the task reward, also referred to as extrinsic reward (Chen et al., 2022). RL algorithms aim to find a policy π^* that maximizes the discounted cumulative reward, i.e.,

$$\pi^* \in \arg \max_{\pi} \mathcal{J}(\pi) := \mathbb{E} \left[\sum_{t=0}^{\infty} \gamma^t r_t \left| \begin{array}{l} s_0 \sim \rho_0, a_t \sim \pi(\cdot | s_t), \\ r_t \sim r(s_t, a_t), s_{t+1} \sim P(\cdot | s_t, a_t) \end{array} \right. \right]. \quad (1)$$

3 METHOD: REWARD DESIGN AS SEQUENTIAL DECISION MAKING

As previously stated, the reward function r encodes the task objective but can be sparse, making it difficult to directly optimize using RL methods. We formalize the reward design problem as follows.

Definition 3.1 (Reward Design). *Let \mathcal{A} be a reinforcement learning algorithm that takes an MDP $\mathcal{M} = (\mathcal{S}, \mathcal{A}, P, r, \gamma, \rho_0)$, a reward function f , and a number of iterations N as input and returns a policy $\pi^f = \mathcal{A}_f(\mathcal{M}, N)$ that approximately maximizes reward f in \mathcal{M} after N iterations.*

Given \mathcal{M} and \mathcal{A} , the reward design problem aims to find a reward function $f : \mathcal{S} \times \mathcal{A} \rightarrow \Delta_{\mathbb{R}}$, with $f \in \mathcal{R}$, the space of reward functions, such that the policy $\pi^f = \mathcal{A}_f(\mathcal{M}, N)$ achieves an expected return under the task reward f , such that $\mathcal{J}(\pi^f) \approx \max_{r' \in \mathcal{R}} \mathcal{J}(\pi^{r'}) = \mathcal{J}(\pi^)$.*

While this could be achieved by running the algorithm \mathcal{A} on every possible reward function $r' \in \mathcal{R}$, this is computationally prohibitive. The reward space \mathcal{R} can be extremely large, and attempting to optimize over all possible rewards is impractical, especially when the available interaction budget is constrained.

To make the problem tractable, we assume access to a finite set of candidate shaping reward functions $\mathcal{R}^K = \{f^1, \dots, f^K\} \sim G(\mathcal{R})$, where G is a distribution over the set of reward functions, that contains at least one near-optimal reward function and a budget of iterations T . If the budget

¹ $\Delta_{\mathcal{S}}$ denotes the set of probability distributions over \mathcal{S} .

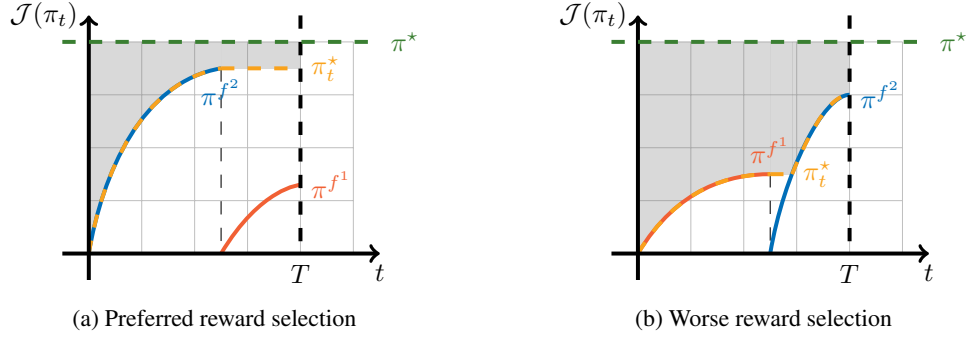


Figure 1: Comparison of two reward selection strategies given a time budget T . The green dashed line represents the task reward of the optimal policy, π^* . The red and blue curves show the cumulative maximum task rewards for policies trained with f^1 and f^2 , respectively. The yellow curve, π_t^* , tracks the maximum of the red and blue curves. The shaded gray area depicts cumulative regret in Equation (2) associated with each selection strategy. The preferred selection strategy, (a), spends most iterations on f^2 , while the worse strategy, which initially focuses on f^1 , leaves too little of the available budget T to fully exploit f^2 , resulting in lower performance and higher regret.

does not allow training on each $f^i \in \mathcal{R}^K$, we need to allocate resources to gather useful information about the quality of each candidate, while simultaneously optimizing the most promising ones. This introduces a fundamental exploration-exploitation tradeoff. On one hand, we must explore various rewards to identify high performers; on the other, we need to exploit promising candidates to train performant policies.

Cumulative Regret \implies Efficiency This tradeoff is captured by a regret-based objective, commonly used in sequential decision-making problems, which measures the suboptimality incurred by the current policy with respect to the optimal one. Therefore, we cast the reward selection problem as an online model selection problem. Let n_t^i denote the number of iterations reward function f^i has been used for training up to iteration t . Then the set of policies trained up to step t is $\Pi(t) = \{\pi_{n_j^i}^{f^{i_j}}\}_{j=1}^t$, where $\pi_{n_j^i}^{f^{i_j}} = \mathfrak{A}_{f^{i_j}}(\mathcal{M}, n_j^i)$, the policy trained with reward function f^{i_j} for n_j^i iterations. We define *practical cumulative regret* as

$$\text{pReg}(T) := \sum_{t=1}^T \mathcal{J}(\pi^*) - \mathcal{J}(\pi_t^*), \quad (2)$$

where $\pi_t^* := \arg \max_{\pi \in \Pi(t)} \mathcal{J}(\pi)$. The choice of π_t^* in the definition of $\text{pReg}(T)$ reflects a practical preference. Practitioners are generally more interested in the best-performing solution available at a given point, rather than the most recent update. For instance, in deploying a robotic running policy, one would select the fastest policy observed thus far – assuming the objective is to run as fast as possible.

The regret minimization framework is well-aligned with the goal of *efficient* reward design, as it emphasizes the speed at which effective policies are learned. In Figure 1, we compare two strategies: one that starts by training with the worse reward function, f^1 , until convergence, and another that immediately focuses on the better reward function, f^2 . The shaded area represents the regret incurred by each selection strategy (Equation (2)), which reflects the performance gap between the learned policy and the optimal one over time. The worse strategy spends too much of the available budget T on f^1 , leaving insufficient iterations for training on f^2 . As a result, the best policy trained with the suboptimal strategy reaches a lower performance and the selection strategy incurs higher regret. Conversely, starting with f^2 minimizes regret and maximizes the performance. A further discussion of the online model selection problem can be found in Appendix B.

3.1 ORSO: ONLINE REWARD SELECTION AND POLICY OPTIMIZATION

In this section, we introduce ORSO (*Online Reward Selection and Optimization*), a novel approach to *efficiently* and *effectively* design reward functions for reinforcement learning. Our method operates in two phases: (1) reward generation and (2) online reward selection and policy optimization.

Reward Generation In the first phase of ORSO, we generate a set of candidate reward functions \mathcal{R}^K for the online selection phase. Given an MDP $\mathcal{M} = (\mathcal{S}, \mathcal{A}, P, r, \rho_0)$ and a stochastic generator G , we sample a set of K reward function candidates, $\mathcal{R}^K = \{f^1, \dots, f^K \mid \forall i \in [K], f^i : \mathcal{S} \times \mathcal{A} \rightarrow \Delta_{\mathbb{R}}, f^i \sim G\}$, from G during the reward design phase. The generator G can be any distribution over the reward function space \mathcal{R} . For instance, if the set of possible reward functions is given by a linear combination of two reward components c_1, c_2 , which are functions of the current state and action, such that $r(s, a) = w_1 c_1(s, a) + w_2 c_2(s, a)$, then the generator G can be represented by the means and variances of two normal distributions, one for each weight w_1, w_2 .

Online Reward Selection and Policy Optimization Our algorithm for online reward selection and policy optimization is described in Algorithm 1. On a high level, the algorithm proceeds as follows. Given an MDP $\mathcal{M} = (\mathcal{S}, \mathcal{A}, P, r, \rho_0)$, an RL algorithm \mathfrak{A} and a reward generator G , we sample set of K reward functions $\mathcal{R}^K \sim G$ and initialize K distinct policies π^1, \dots, π^K . At step t of the reward selection process, the algorithm selects a learner $i_t \in [K]$ according to a selection strategy. We then perform N iterations of training with algorithm \mathfrak{A} , updating the policy corresponding to reward function i_t to obtain π^{i_t} . Policy π^{i_t} is simultaneously evaluated under the task reward function r and the necessary variables for the model selection algorithm are then updated (e.g., reward estimates, reward function visitation counts, and confidence intervals). The algorithm returns the reward function f_T^* and the corresponding policy π_T^* that performs the best under the task reward function r .

Algorithm 1 ORSO: Online Reward Selection and Policy Optimization

Require: MDP $\mathcal{M} = (\mathcal{S}, \mathcal{A}, P, r, \rho_0)$, algorithm \mathfrak{A} , generator G

- 1: Sample K reward functions $\mathcal{R}^K = \{f^1, \dots, f^K\} \sim G$
- 2: Initialize K policies $\{\pi^1, \dots, \pi^K\}$
- 3: **for** $t = 1, 2, \dots, T$ **do**
- 4: Select an model $i_t \in [K]$ according to a selection strategy
- 5: Update $\pi^{i_t} \leftarrow \mathfrak{A}_{f^{i_t}}(\mathcal{M}, N, \pi^{i_t})$
- 6: Evaluate $\mathcal{J}(\pi^{i_t}) \leftarrow \text{Eval}(\pi^{i_t})$
- 7: Update variables (e.g., reward estimates and confidence intervals)
- 8: **end for**
- 9: **return** $\pi_T^*, f_T^* = \arg \max_{i \in [K]} \mathcal{J}(\pi^i)$

Choice of Selection Algorithm While ORSO is a general algorithm that can employ any selection method to pick the reward function to train on, the performance depends on the choice of algorithm.

For instance, using a simple selection method like ε -greedy introduces an element of exploration by occasionally selecting a random reward function (with probability ε), but it risks overcommitting to a seemingly promising reward function early on. This can lead to suboptimal performance if the chosen reward function causes the task performance to plateau in the long run. However, greedier methods, such as ε -greedy, can achieve lower regret if they commit to the actual optimal reward function early in the process. These methods are particularly effective when early performance signals are strong indicators of long-term success.

However, if initial performance is not a reliable predictor of future outcomes, these greedy approaches may struggle, as they risk prematurely locking onto suboptimal rewards. In contrast, more exploratory algorithms like the exponential-weight algorithm for exploration and exploitation (Exp3) (Auer et al., 2002) maintain a broader search, potentially discovering better rewards in the long run, especially in environments where early signals are less informative. We empirically validate different choices of selection algorithms in Section 5.

4 THEORETICAL GUARANTEES

In this section, we provide regret guarantees for ORSO with the Doubling Data-Driven Regret Balancing (D³RB) algorithm by Dann et al. (2024). A discussion of the intuition behind the D³RB algorithm and the full pseudo-code for ORSO with D³RB is provided in Appendix C. We note that the regret definition used in the online model selection literature is an upper bound for the practical cumulative regret defined in Section 3. We provide a further discussion of this relationship in Appendix B.

We first introduce some useful definitions for our analysis.

Definition 4.1 (Definition 2.1 from Dann et al. (2024)). *The regret scale of learner i after being played t times is $\frac{\sum_{\ell=1}^t \text{reg}(\pi_{(\ell)}^i)}{\sqrt{t}}$ where $\text{reg}(\pi_{(\ell)}^i) = \mathcal{J}(\pi^*) - \mathcal{J}(\pi_{(\ell)}^i)$ in the reward design problem.*

For a positive constant $d_{\min} > 0$, the regret coefficient of learner i after being played for t rounds is $d_{(t)}^i = \max\{d_{\min}, \sum_{\ell=1}^t \text{reg}(\pi_{(\ell)}^i)/\sqrt{t}\}$. That is, $d_{(t)}^i \geq d_{\min}$ is the smallest number such that the incurred regret is bounded as $\sum_{\ell=1}^t \text{reg}(\pi_{(\ell)}^i) \leq d_{(t)}^i \sqrt{t}$.

Dann et al. (2024) use \sqrt{t} as this is the most commonly targeted regret rate in stochastic settings.

The main idea underlying our regret guarantees is that the internal state of all suboptimal reward functions is only updated up to a point where the regret equals that of the best policy so far.

We assume there exists a learner that monotonically dominates every other learner.

Assumption 4.2. *There is a learner i_* such that at all time steps, its expected sum of rewards dominates any other learner, i.e., $u_{(t)}^{i_*} \geq u_{(t)}^i$, for all $i \in [K], t \in \mathbb{N}$ and such that its average expected rewards are increasing, i.e., $\frac{u_{(t)}^{i_*}}{t} \leq \frac{u_{(t+1)}^{i_*}}{t+1}$, $\forall t \in \mathbb{N}$. This is equivalent to saying that $d_{(t)}^{i_*} \geq d_{(t+1)}^{i_*}$, for all $t \in \mathbb{N}$.*

Assumption 4.2 guarantees that the cumulative expected reward of the optimal learner i_* is always at least as large as the cumulative expected reward of any other learner and that its average performance increases monotonically.

Following the notation of Dann et al. (2024), we refer to the event that the confidence intervals for the reward estimator are valid as \mathcal{E} .

Definition 4.3 (Definition 8.1 from Dann et al. (2024)). *We define the event \mathcal{E} as the event in which for all rounds $t \in \mathbb{N}$ and learners $i \in [K]$ the following inequalities hold*

$$-c\sqrt{n_t^i \ln \frac{K \ln n_t^i}{\delta}} \leq \hat{u}_t^i - u_t^i \leq c\sqrt{n_t^i \ln \frac{K \ln n_t^i}{\delta}} \quad (3)$$

for the algorithm parameter $\delta \in (0, 1)$ and a universal constant $c > 0$.

Then we can refine Lemma 9.3 from Dann et al. (2024) in the case where Assumption 4.2 holds.

Lemma 4.4. *Under event \mathcal{E} and Assumption 4.2, with probability $1 - \delta$, the regret of all learners i is bounded in all rounds T as*

$$\sum_{t=1}^{n_T^i} \text{reg}(\pi_{(t)}^i) \leq 6d_T^{i_*} \sqrt{n_T^{i_*} + 1} + 5c\sqrt{(n_T^{i_*} + 1) \ln \frac{K \ln T}{\delta}}, \quad (4)$$

where $d_T^{i_*} = d_{(n_T^{i_*})}^{i_*}$.

We provide the proof for Lemma 4.4 in Appendix D. Lemma 4.4 implies that when Assumption 4.2 holds, the regrets are perfectly balanced. This is in stark contrast with the regret guarantees of Dann et al. (2024) that prove the D³RB algorithm's overall regret to scale as $(\bar{d}_T^{i_*})^2 \sqrt{T}$ where $\bar{d}_t^{i_*} = \max_{\ell \leq t} d_{(\ell)}^{i_*}$. Instead, our results above depend not on the monotonic regret coefficients $\bar{d}_t^{i_*}$ but on the true regret coefficients $d_t^{i_*}$. Even if learner i_* has a slow start (and therefore a large $\bar{d}_T^{i_*}$), as long as monotonicity holds and the i_* -th learner recovers in the later stages of learning, our results show that D³RB will achieve a regret guarantee comparable with running learner i_* in isolation.

5 PRACTICAL IMPLEMENTATION AND EXPERIMENTAL RESULTS

In this section, we present a practical implementation² of ORSO and its experimental results on several continuous control tasks. We study the ability of ORSO to design effective reward functions with varying budget constraints. We also study how different sample sizes, K , of the set of reward functions \mathcal{R}^K influence the performance of ORSO and compare different selection algorithms.

This section is structured as follows. First, we present the experimental setup, including the environments and baselines, and the practical consideration of the reward generator G and the algorithms used in the online reward selection phase. Then, we present the main results and ablate our design choices. Further experimental results can be found in Appendix H

5.1 EXPERIMENTAL SETUP

Environments and RL Algorithm We evaluate ORSO on a set of continuous control tasks using the Isaac Gym simulator (Makoviychuk et al., 2021). Specifically, we consider the following tasks: CARPOLE and BALLBALANCE, which are relatively simple; two locomotion tasks, ANT and HUMNAOID, which have dense but unshaped task rewards – for instance, the agent is rewarded for running fast, but the reward function lacks terms to encourage upright posture or smooth movement; and two complex manipulation tasks, ALLEGROHAND and SHADOWHAND, which feature sparse task reward functions.

Our policies are trained using the proximal policy optimization (PPO) algorithm (Schulman et al., 2017), with our implementation built on CleanRL (Huang et al., 2022). We chose PPO because the Makoviychuk et al. (2021) provide hyperparameters, which we use, that enable it to perform well on these tasks when using the human-engineered reward functions.

5.1.1 BASELINES

In our experiments, we consider three baselines. We analyze the performance of policies trained using each reward function detailed below. We evaluate the reward function selection *efficiency* of ORSO compared to more naive selection strategies.

No Design (*Task Reward with No Shaping*) We train the agent with the task reward function r for each MDP. These reward functions can be sparse (for manipulation) or unshaped (for locomotion). We use the same reward definitions as prior work (Ma et al., 2024), which we report in Appendix E.

Human We consider the human-engineered reward functions for each task provided by (Makoviychuk et al., 2021). We note that these are constructed such that training PPO with the given hyperparameters yields a performant policy with respect to the task reward function. The function definitions are reported in Appendix E.

Naive Selection We employ EUREKA (Ma et al., 2024) as a baseline for the naive selection approach. EUREKA uses a large language model to generate Python code for the reward functions of several continuous control tasks. EUREKA uses an evolutionary scheme to evaluate and improve its reward functions. During each iteration, EUREKA samples a set of reward functions from an LLM, trains a policy on each reward function, and uses the best-performing reward function as a context for the LLM to perform the evolutionary step. However, this selection strategy can be seen as naive, as it uniformly explores each reward function for a fixed number of iterations, regardless of its actual performance on the task.

5.1.2 IMPLEMENTATION

Reward Generation Similarly to recent works on reward design, which demonstrate that LLMs can generate effective reward functions for training agents (Park et al., 2024; Ma et al., 2024; Xie et al., 2024), we follow this paradigm by using GPT-4 (Achiam et al., 2023) to avoid manually designing reward function components. The language model is prompted to generate reward function

²The code for ORSO is available at <https://github.com/calvincbzhang/orso>

code in Python based on some minimal environment code describing the observation space and useful class variables. We employ prompts similar to those used by Ma et al. (2024). Since the exact prompts are not the primary focus of our work, we do not detail them here; instead, we refer readers to our codebase for further details on the prompt construction.

While the LLM produces seemingly good code, this does not guarantee that the sampled code is bug-free and runnable. In ORSO, we employ a simple rejection sampling technique to construct sets of only valid reward functions with high probability. We also note that the initial set of generated reward functions in ORSO might not contain an effective reward function.³ To address this limitation, we introduce a mechanism for improving the reward function set through iterative resampling and in-context evolution of new sets \mathcal{R}^K . We provide more details on the rejection sampling mechanism and the iterative refinement process Appendix F.

Online Reward Selection Algorithms We evaluate multiple reward selection algorithms from the multi-armed bandit and online model selection literature: explore-then-commit (ETC), ϵ -greedy (EG), upper confidence bound (UCB) (Auer, 2002), exponential-weight algorithm for exploration and exploitation (EXP3) (Auer et al., 2002), and doubling data-driven regret balancing (D3RB) (Dann et al., 2024). We provide the pseudocode and the hyperparameters used for each selection algorithm in Appendix G. For every environment, we set the number of iterations N in Algorithm 1 used to train the policy before we select a different reward function to $N = \text{n_iters}/100$, where n_iters is the number of iterations used to train with the human-engineered reward function, i.e., we perform at least 100 iterations of online reward selection before the iterative resampling.

5.2 RESULTS

In this section, we present the experimental results of ORSO. We evaluate ORSO’s ability to efficiently select reward functions with varying budget constraints and reward function set size K . We consider budgets $B \in \{5, 10, 15\} \times \text{n_iters}$ and sample sizes $K \in \{4, 8, 16\}$.

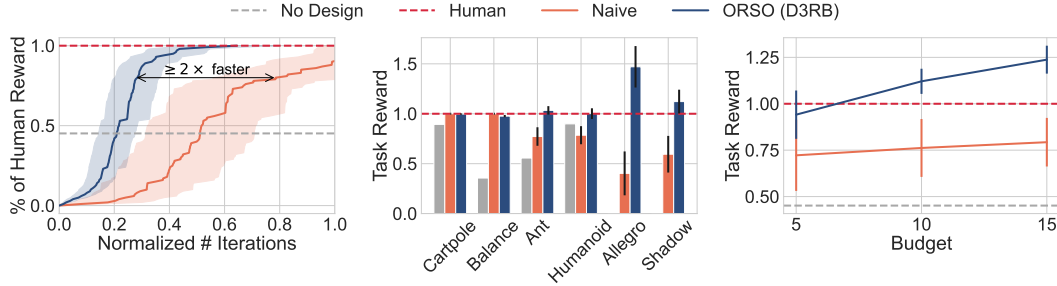


Figure 2: **Left:** ORSO achieves human-level performance in approximately half the time compared to the naive strategy. The curves represent the average percentage of human-designed reward functions across multiple tasks and iteration budget constraints. **Middle:** Normalized task rewards averaged over various iteration budgets and seeds. ORSO consistently matches or surpasses human-designed reward functions. The normalized task reward is averaged over different iteration budgets and seeds. **Right:** Normalized task rewards across different iteration budgets. ORSO effectively scales with increased iterations, with values averaged over multiple tasks and seeds. Shaded areas and vertical bars in the plots indicate 95% confidence intervals.

ORSO is Twice as Fast as the Naive Selection Strategy In Figure 2 (left), we plot the number of iterations required to reach different percentages of the performance achieved by policies trained with human-engineered reward functions. The y-axis represents the percentage of human performance, while the x-axis shows progress in the selection algorithm, normalized so that a value of 1.0 corresponds to $B \times \text{n_iters}$ for each task. Results are aggregated across 6 tasks, 3 different budgets, and 3 reward function sets, with 3 seeds per configuration, totaling 162 runs.

³An effective reward function is one that leads to high performance with respect to the task reward r when used for training.

We observe that ORSO with D³RB achieves human-level performance more than twice as fast as the naive selection strategy. The naive selection strategy on average does not manage to select an effective reward function within the limited budget. Detailed per-task and per-budget results are reported in Appendix H.

ORSO Surpasses Human-Designed Reward Functions Not only does ORSO reach human-level performance quickly, but it also has the potential to surpass it. Figure 2 (middle) illustrates the average performance of ORSO compared to human-designed reward functions, the task reward function, and the naive selection strategy across different tasks. We observe that ORSO consistently matches or exceeds human-designed rewards, particularly in more complex environments. Again, the results are averaged over multiple seeds and configurations. The full breakdown is reported in Appendix H.

ORSO Scales with Budget Figure 2 (right) demonstrates how ORSO’s performance scales with increasing budgets. While both ORSO and naive selection benefit from larger budgets, ORSO is consistently superior and surpasses human-designed rewards when $B \geq 10$.

5.3 ABLATION STUDY

Choice of Selection Algorithm In Figure 3, we compare different selection algorithms for ORSO. We find that D³RB performs best on average, consistently outperforming other algorithms, followed closely by Exp3. These algorithms allow ORSO to balance exploration and exploitation effectively, leading to superior performance compared to more greedy approaches like UCB, ETC, and EG. Interestingly, even simpler strategies like EG and ETC substantially outperform the naive strategy, which highlights the importance of properly balancing exploration and exploitation for efficient reward selection. By framing reward design as an exploration-exploitation problem, we demonstrate that even basic strategies offer considerable gains over static, inefficient methods.

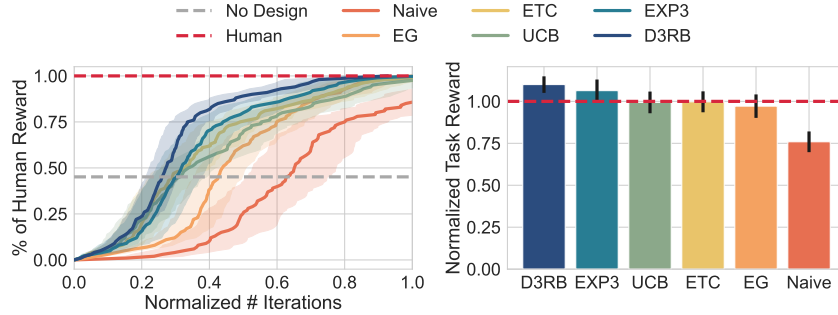


Figure 3: Comparison of different rewards selection algorithms for ORSO. **Left:** Number of iterations necessary for human-level performance. **Right:** Average normalized task reward for different selection algorithms. We provide a more granular breakdown in Appendix H.

Regret of Different Selection Algorithms To further quantify ORSO’s performance, we analyze its regret with respect to human-engineered reward functions.⁴ This formulation is motivated by two key considerations. First, we lack access to the true optimal policy π^* . Second, the PPO hyperparameters used in our experiments were specifically tuned for the human-engineered reward function, making the policy trained with it a reasonable proxy for the optimal policy. Regret provides a useful metric for understanding how much performance is lost due to suboptimal reward selection over time. Lower regret indicates that ORSO quickly identifies high-quality reward functions, reducing the number of iterations wasted on poorly performing ones. Figure 4 shows the normalized cumulative regret for different selection algorithms. Notably, ORSO’s regret can become negative, indicating that it finds reward functions that outperform the human baseline.

⁴The normalized cumulative regret with respect to the human-engineered reward functions is defined as $\frac{1}{T} \sum_{t=1}^T \frac{\text{Human} - \mathcal{J}(\pi_t^*)}{\text{Human}}$.

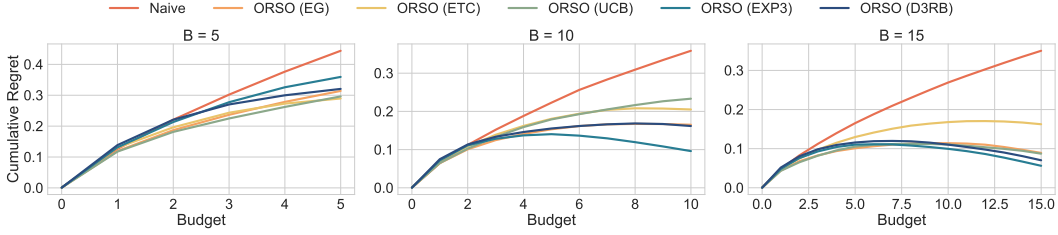


Figure 4: Regret of different selection algorithms with varying budgets. We recall that a budget B indicates that the ORSO has been run for $B \times \text{n_iters}$ iterations.

ORSO is Effective with Large Reward Sets We also evaluate ORSO with different selection algorithms when we are provided with a fixed but large set of reward functions. Specifically, we conduct experiments on the ANT task using ORSO with a budget $B = 15$ and candidate shaping reward sets of sizes $K \in \{48, 96\}$.

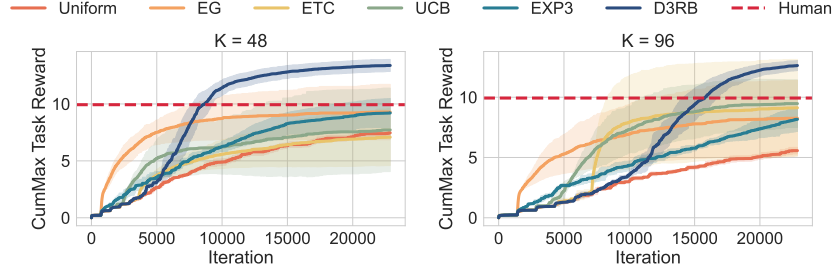


Figure 5: Comparison of multiple selection algorithms for the ANT task with a high number of reward function candidates. The shaded areas represent 95% confidence intervals over 5 different seeds. The order of the reward functions is randomized for each seed.

In this setting – with a fixed budget, but no iterative improvement – algorithms that commit to a selection earlier can allocate more iterations to training on the chosen reward functions. On the other hand, exploring for longer may allow us to find the optimal reward function but potentially leave insufficient time for training.

As illustrated in Figure 5, D³RB consistently identifies and selects an effective reward function from the set. In contrast, “greedier” methods such as ϵ -greedy, explore-then-commit, and UCB can depend more on the stochasticity of training and on average do not surpass human-designed reward functions. Exp3 and uniform exploration, while more exploratory, may overemphasize exploration at the expense of exploiting promising reward functions, leading to suboptimal performance.

6 CONCLUSION

In this paper, we introduce ORSO, a novel approach for reward design in reinforcement learning that significantly accelerates the design of shaped reward functions. We find that even simple strategies like ϵ -greedy and explore-then-commit yield substantial improvements over naive selection, suggesting that reward design can be effectively framed as a sequential decision problem. ORSO reduces both time and computational costs by more than half compared to earlier methods, making reward design accessible to a wider range of researchers. By formalizing the reward design problem and providing a theoretical analysis of ORSO’s regret when using the D³RB algorithm, we also contribute to the theoretical understanding of reward design in RL.

Looking ahead, our work opens several promising directions for future research, including the development of more sophisticated exploration strategies tailored for reward design, and the application of our approach to more complex, real-world RL problems.

6.1 LIMITATIONS AND FUTURE WORK

A key limitation of ORSO is its reliance on a predefined task reward, which is typically straightforward to construct for simpler tasks but can be challenging for more complex ones or for tasks that include a qualitative element to them, e.g., making a quadruped walk with a “nice” gait. Future work could explore eliminating the need for such hand-crafted task rewards by leveraging techniques that translate natural language instructions directly into evaluators, potentially using vision-language models, similarly to Wang et al. (2024); Rocamonde et al. (2024). Another alternative is to use preference data to learn a task reward model (Christiano et al., 2017; Zhang & Ramponi, 2023) and use the latter as a signal for the model selection algorithm.

ACKNOWLEDGEMENTS

We thank members of the Improbable AI Lab for helpful discussions and feedback. We are grateful to MIT Supercloud and the Lincoln Laboratory Supercomputing Center for providing HPC resources. This research was supported in part by Hyundai Motor Company, Quanta Computer Inc., an AWS MLRA research grant, ARO MURI under Grant Number W911NF-23-1-0277, DARPA Machine Common Sense Program, ARO MURI under Grant Number W911NF-21-1-0328, and ONR MURI under Grant Number N00014-22-1-2740. The views and conclusions contained in this document are those of the authors and should not be interpreted as representing the official policies, either expressed or implied, of the Army Research Office or the United States Air Force or the U.S. Government. The U.S. Government is authorized to reproduce and distribute reprints for Government purposes, notwithstanding any copyright notation herein.

AUTHOR CONTRIBUTIONS

- **Chen Bo Calvin Zhang:** Led the project, wrote the manuscript, ideated the method, implemented the algorithm, and conducted the experiments.
- **Zhang-Wei Hong:** Provided guidance on the types of experiments to run and assisted with the implementation of saving and loading the simulator state in Isaac Gym. Drafted the introduction and advised on writing.
- **Aldo Pacchiano:** Contributed to the theoretical aspects of the work, specifically the model selection part, including the development and proof of key concepts.
- **Pulkit Agrawal:** Oversaw the project, assisted with positioning the paper, and contributed to the writing and presentation of the results.

REFERENCES

- Pieter Abbeel and Andrew Y Ng. Apprenticeship learning via inverse reinforcement learning. In *Proceedings of the twenty-first international conference on Machine learning*, pp. 1, 2004.
- Josh Achiam, Steven Adler, Sandhini Agarwal, Lama Ahmad, Ilge Akkaya, Florencia Leoni Aleman, Diogo Almeida, Janko Altschmidt, Sam Altman, Shyamal Anadkat, et al. GPT-4 technical report. *arXiv preprint arXiv:2303.08774*, 2023.
- Alekh Agarwal, Haipeng Luo, Behnam Neyshabur, and Robert E Schapire. Corraling a band of bandit algorithms. In *Conference on Learning Theory*, pp. 12–38. PMLR, 2017.
- Pulkit Agrawal. The task specification problem. In *5th Annual Conference on Robot Learning, Blue Sky Submission Track*, 2021. URL <https://openreview.net/forum?id=cBdnThrYkV7>.
- Peter Auer. Using confidence bounds for exploitation-exploration trade-offs. *Journal of Machine Learning Research*, 3(Nov):397–422, 2002.
- Peter Auer, Nicolo Cesa-Bianchi, Yoav Freund, and Robert E Schapire. The nonstochastic multi-armed bandit problem. *SIAM journal on computing*, 32(1):48–77, 2002.

- Ralph Allan Bradley and Milton E Terry. Rank analysis of incomplete block designs: I. the method of paired comparisons. *Biometrika*, 39(3/4):324–345, 1952.
- Eric R Chen, Zhang-Wei Hong, Joni Pajarinen, and Pulkit Agrawal. Redeeming intrinsic rewards via constrained policy optimization. In Alice H. Oh, Alekh Agarwal, Danielle Belgrave, and Kyunghyun Cho (eds.), *Advances in Neural Information Processing Systems*, 2022. URL https://openreview.net/forum?id=36Yz37cEN_Q.
- Paul F Christiano, Jan Leike, Tom Brown, Miljan Martic, Shane Legg, and Dario Amodei. Deep reinforcement learning from human preferences. *Advances in neural information processing systems*, 30, 2017.
- Chris Dann, Claudio Gentile, and Aldo Pacchiano. Data-driven online model selection with regret guarantees. In *International Conference on Artificial Intelligence and Statistics*, pp. 1531–1539. PMLR, 2024.
- Dylan J Foster, Akshay Krishnamurthy, and Haipeng Luo. Model selection for contextual bandits. *Advances in Neural Information Processing Systems*, 32, 2019.
- Shengyi Huang, Rousslan Fernand Julien Dossa, Chang Ye, Jeff Braga, Dipam Chakraborty, Kinal Mehta, and Joˆˆo GM Araˆˆsjo. Cleanrl: High-quality single-file implementations of deep reinforcement learning algorithms. *Journal of Machine Learning Research*, 23(274):1–18, 2022.
- Martin Klissarov, Pierluca D’Oro, Shagun Sodhani, Roberta Raileanu, Pierre-Luc Bacon, Pascal Vincent, Amy Zhang, and Mikael Henaff. Motif: Intrinsic motivation from artificial intelligence feedback. In *The Twelfth International Conference on Learning Representations*, 2024. URL <https://openreview.net/forum?id=tmBKIEcDE9>.
- Minae Kwon, Sang Michael Xie, Kalesha Bullard, and Dorsa Sadigh. Reward design with language models. In *The Eleventh International Conference on Learning Representations*, 2023. URL <https://openreview.net/forum?id=10uNUgI5Kl>.
- Jonathan Lee, Aldo Pacchiano, Vidya Muthukumar, Weihao Kong, and Emma Brunskill. Online model selection for reinforcement learning with function approximation. In *International Conference on Artificial Intelligence and Statistics*, pp. 3340–3348. PMLR, 2021.
- Minghuan Liu, Zixuan Chen, Xuxin Cheng, Yandong Ji, Ri-Zhao Qiu, Ruihan Yang, and Xiaolong Wang. Visual whole-body control for legged loco-manipulation. In *8th Annual Conference on Robot Learning*, 2024. URL <https://openreview.net/forum?id=cT2N3p1AcE>.
- Yecheng Jason Ma, William Liang, Guanzhi Wang, De-An Huang, Osbert Bastani, Dinesh Jayaraman, Yuke Zhu, Linxi Fan, and Anima Anandkumar. Eureka: Human-level reward design via coding large language models. In *The Twelfth International Conference on Learning Representations*, 2024. URL <https://openreview.net/forum?id=IEduRU055F>.
- A Rupam Mahmood, Dmytro Korenkevych, Gautham Vasan, William Ma, and James Bergstra. Benchmarking reinforcement learning algorithms on real-world robots. In *Conference on robot learning*, pp. 561–591. PMLR, 2018.
- Viktor Makoviychuk, Lukasz Wawrzyniak, Yunrong Guo, Michelle Lu, Kier Storey, Miles Macklin, David Hoeller, Nikita Rudin, Arthur Allshire, Ankur Handa, and Gavriel State. Isaac gym: High performance GPU based physics simulation for robot learning. In *Thirty-fifth Conference on Neural Information Processing Systems Datasets and Benchmarks Track (Round 2)*, 2021. URL https://openreview.net/forum?id=fgFBtYgJQX_.
- Gabriel B. Margolis and Pulkit Agrawal. Walk these ways: Tuning robot control for generalization with multiplicity of behavior. In *6th Annual Conference on Robot Learning*, 2022. URL <https://openreview.net/forum?id=52c5e73S1S2>.
- Andrew Y Ng, Daishi Harada, and Stuart Russell. Policy invariance under reward transformations: Theory and application to reward shaping. In *Icml*, volume 99, pp. 278–287, 1999.

- Aldo Pacchiano, My Phan, Yasin Abbasi Yadkori, Anup Rao, Julian Zimmert, Tor Lattimore, and Csaba Szepesvari. Model selection in contextual stochastic bandit problems. *Advances in Neural Information Processing Systems*, 33:10328–10337, 2020.
- Younghyo Park, Gabriel B. Margolis, and Pulkit Agrawal. Position: Automatic environment shaping is the next frontier in RL. In *Forty-first International Conference on Machine Learning*, 2024. URL <https://openreview.net/forum?id=dslUyy1rN4>.
- Martin L Puterman. *Markov decision processes: discrete stochastic dynamic programming*. John Wiley & Sons, 2014.
- Juan Rocamonde, Victoriano Montesinos, Elvis Nava, Ethan Perez, and David Lindner. Vision-language models are zero-shot reward models for reinforcement learning. In *The Twelfth International Conference on Learning Representations*, 2024. URL <https://openreview.net/forum?id=N0I2RtD8je>.
- John Schulman, Filip Wolski, Prafulla Dhariwal, Alec Radford, and Oleg Klimov. Proximal policy optimization algorithms. *arXiv preprint arXiv:1707.06347*, 2017.
- Richard S Sutton and Andrew G Barto. *Reinforcement learning: An introduction*. MIT press, 2018.
- Yufei Wang, Zhanyi Sun, Jesse Zhang, Zhou Xian, Erdem Biyik, David Held, and Zackory Erickson. RL-VLM-f: Reinforcement learning from vision language foundation model feedback. In *Forty-first International Conference on Machine Learning*, 2024. URL <https://openreview.net/forum?id=YSOMmNWZZx>.
- Tianbao Xie, Siheng Zhao, Chen Henry Wu, Yitao Liu, Qian Luo, Victor Zhong, Yanchao Yang, and Tao Yu. Text2reward: Reward shaping with language models for reinforcement learning. In *The Twelfth International Conference on Learning Representations*, 2024. URL <https://openreview.net/forum?id=tUM39YTRxH>.
- Wenhao Yu, Nimrod Gileadi, Chuyuan Fu, Sean Kirmani, Kuang-Huei Lee, Montserrat Gonzalez Arenas, Hao-Tien Lewis Chiang, Tom Erez, Leonard Hasenclever, Jan Humplik, Brian Ichter, Ted Xiao, Peng Xu, Andy Zeng, Tingnan Zhang, Nicolas Heess, Dorsa Sadigh, Jie Tan, Yuval Tassa, and Fei Xia. Language to rewards for robotic skill synthesis. In *7th Annual Conference on Robot Learning*, 2023. URL <https://openreview.net/forum?id=SgTPdyehXMA>.
- Chen Bo Calvin Zhang and Giorgia Ramponi. HIP-RL: Hallucinated inputs for preference-based reinforcement learning in continuous domains. In *ICML 2023 Workshop The Many Facets of Preference-Based Learning*, 2023. URL <https://openreview.net/forum?id=PRm1KxRrWI>.
- Brian D Ziebart, Andrew L Maas, J Andrew Bagnell, Anind K Dey, et al. Maximum entropy inverse reinforcement learning. In *Aaai*, volume 8, pp. 1433–1438. Chicago, IL, USA, 2008.

A RELATED WORK

Reward Design for RL Designing effective reward functions for reinforcement learning has been a long-standing challenge. Several approaches have been proposed to tackle it.

Traditionally, researchers manually specify reward components and tune their coefficients (Ng et al., 1999; Margolis & Agrawal, 2022; Liu et al., 2024). This method often demands significant domain expertise and can be highly resource-intensive, involving numerous iterations of trial and error in designing reward functions, training policies, and adjusting reward parameters.

Another approach is to learn reward functions from expert demonstrations via methods like apprenticeship learning (Abbeel & Ng, 2004) and maximum entropy inverse RL (Ziebart et al., 2008). While these methods can capture complex behaviors, they often rely on high-quality demonstrations and may struggle in environments where such data is scarce or noisy.

Preferences can also be used to learn reward functions (Zhang & Ramponi, 2023; Christiano et al., 2017). This approach involves collecting feedback in the form of preferences between different trajectories, which are then used to infer a reward function that aligns with the desired behavior. This method is particularly useful in scenarios where it is difficult to explicitly define a reward function or obtain expert demonstrations, as it allows for more intuitive and accessible feedback from users.

Foundation Models and Reward Functions Recent work has explored the use of large language/vision models (LL/VMs) to aid in the reward design process. L2R (Yu et al., 2023) leverages large language models to generate reward functions for RL tasks by first creating a natural language “motion description” and then converting it into code using predefined reward API primitives. While innovative, L2R has notable limitations: it requires significant manual effort in designing templates and primitives and is constrained by the latter. EUREKA (Ma et al., 2024) and Text2Reward (Xie et al., 2024) use LLMs to generate dense reward functions for RL given the task description in natural language and the environment code.

Foundation models have also been directly used as reward models. Rocamonde et al. (2024) uses the cosine similarity of CLIP embeddings of language instructions and renderings of the state as a state-only reward model. Similarly, Wang et al. (2024) automatically generates reward functions for RL using a vision language model to label pairs of trajectories with preference, given a task description. Motif (Klissarov et al., 2024) first constructs a pair-wise preferences dataset using a large language model (LLM), learns a preference-based intrinsic reward model with the Bradley-Terry (Bradley & Terry, 1952) model, and then uses this reward model to train a reinforcement learning agent. Kwon et al. (2023) uses a similar approach, where an LLM is used during training to evaluate an RL policy, given a few examples of successful behavior or a description of the desired behavior.

Online Model Selection The problem of model selection in sequential decision-making environments has gained significant attention in recent years (Agarwal et al., 2017; Foster et al., 2019; Pacchiano et al., 2020; Lee et al., 2021). This area of research addresses the challenge of dynamically choosing the most suitable model or algorithm from a set of candidates while learning.

Agarwal et al. (2017) introduced CORRAL, a method to combine multiple bandit algorithms in a master algorithm. Foster et al. (2019) proposed model selection guarantees for linear contextual bandits. Pacchiano et al. (2020) extend the CORRAL algorithm and propose Stochastic CORRAL. Lastly, Lee et al. (2021) propose Explore-Commit-Eliminate (ECE), an algorithm for model selection in RL with function approximation. A common requirement across all these approaches is the need to know the regret guarantees of the base algorithms.

Our work is closely related to Dann et al. (2024), which removes the need for known regret guarantees and instead uses *realized* regret bounds for the base learners. In our setting, the set of models comprises the reward functions set and their corresponding policies.

B ONLINE MODEL SELECTION

In this section, we introduce the model selection problem and some necessary notation modified from Dann et al. (2024) for our analysis.

We consider a general sequential decision-making process consisting of a *meta learner* interacting with an environment over $T \in \mathbb{N}$ rounds via a set of *base learners*. At each round of interaction $t = 1, 2, \dots, T$, the meta learner selects a base learner b_t and after executing b_t , the environment returns a model selection reward $R_t \in \mathbb{R}$. The objective of the meta learner is to sequentially choose base learners b_1, \dots, b_T to maximize the expected cumulative sum of model selection rewards, i.e., $\max \mathbb{E} \left[\sum_{t=1}^T R_t \right]$. We denote by $v^b = \mathbb{E}[R \mid b]$ the expected model selection reward, given that the learner chooses base learner b , i.e., the value of base learner b . The total model selection reward accumulated by the algorithm over T rounds is denoted by $u_T = \sum_{t=1}^T v^{b_t}$. The objective is to minimize the cumulative regret after T rounds of interaction,

$$\text{Reg}(T) := \sum_{t=1}^T \text{reg}(b_t) = \sum_{t=1}^T v^* - v^{b_t}, \quad (5)$$

where v^* is the value of the optimal base learner.

In our setting, each base learner corresponds to a reward function r and its associated policy π , i.e., $b = (f, \pi)$. In this case, choosing to execute base learner b means training with algorithm \mathfrak{A} starting from checkpoint π and using RL reward function f . The model selection reward R is then the evaluation of the trained policy under the task reward r , i.e., $\mathcal{J}(\pi)$. The regret of base learner b can therefore be written as $\text{reg}(b) = v^* - v^b = \mathcal{J}(\pi^*) - \mathcal{J}(\pi)$, where π^* is the optimal policy. Therefore the objective becomes minimizing

$$\text{Reg}(T) = \sum_{t=1}^T \mathcal{J}(\pi^*) - \mathcal{J}(\pi_{n_t^{i_t}}^{f^{i_t}}). \quad (6)$$

We note an important difference between the online model selection problem and the multi-armed bandit (MAB) problem. In model selection, the meta learner interacts with an environment over T rounds, selecting from K base learners. In each round t , the meta learner picks a base learner $i_t \in [K]$ (index of base learner chosen at step t) and follows its policy, updating the base learner's state with new data. Unlike MAB problems, where mean rewards are stationary, the mean rewards here are non-stationary due to the stateful nature of base learners (the base learners are learning as they see more data), making the design of effective model selection algorithms challenging.

Notation The policy associated with base learner i at round t is denoted by π_t^i , so that $\pi_t = \pi_t^{i_t}$. We denote the number base learner i has been played up to round t as $n_t^i = \sum_{\ell=1}^t \mathbb{1}\{i_\ell = i\}$ and the total cumulative reward for learner i as $u_t^i = \sum_{\ell=1}^t \mathbb{1}\{i_\ell = i\} v^{\pi_\ell^i}$, where we use $v^{\pi_\ell^i} = v^{b_\ell^i}$ to highlight that the policy associated with base learner i changes over time, but the reward function used for RL does not. We denote the internal clock for each base learner with a subscript (k) such that $\pi_{(k)}^i$ is the policy of learner i when chosen for the k -th time, i.e., $\pi_t^i = \pi_{(n_t^i)}^i$.

Remark 1. The cumulative regret in Equation (6) is an upper bound for the practical cumulative regret.

Proof. This is straightforward to see. Let us first note that, by definition, for all $t \in [T]$, we have

$$\mathcal{J}(\pi_t^*) \geq \mathcal{J}(\pi_{n_t^{i_t}}^{f^{i_t}}). \quad (7)$$

Therefore,

$$\sum_{t=1}^T \mathcal{J}(\pi^*) - \mathcal{J}(\pi_t^*) \leq \sum_{t=1}^T \mathcal{J}(\pi^*) - \mathcal{J}(\pi_{n_t^{i_t}}^{f^{i_t}}), \quad (8)$$

i.e.,

$$\text{pReg}(T) \leq \text{Reg}(T), \quad (9)$$

concluding the proof. \square

C ORSO WITH DOUBLING DATA-DRIVEN REGRET BALANCING

Here, we present the complete ORSO algorithm with Doubling Data-Driven Regret Balancing (D³RB) as the model selection algorithm.

D³RB is built upon the idea of *regret balancing*, which aims to optimize the performance of multiple models by balancing their respective regrets. Imagine weighing two models on a balance scale where the “weight” corresponds to their regret; the goal is to keep the regret of both models balanced. This approach ensures that models with higher regret rates are selected less frequently, while those with lower regret rates are favored.

Concretely, regret balancing involves associating each learner with a candidate regret bound. The model selection algorithm then competes against the regret bound of the best-performing learner among those that are well-specified – meaning their realized regret stays within their candidate bounds. Traditional approaches often rely on known *expected* regret bounds. In contrast, D³RB focuses on *realized* regret, allowing the model selection algorithm to compete based on the actual regret outcomes of each base learner. The algorithm dynamically adjusts the regret bounds in a data-driven manner, adapting to the realized regret of the best-performing learner over time. This approach overcomes the limitation of needing known regret bounds, which are often unavailable for complex problems.

D³RB maintains three estimators for each base learner: regret coefficients \hat{d}_t^i , average rewards \hat{u}_t^i/n_t^i and balancing potentials ϕ_t^i . At each step t , D³RB selects the base learner with the lower balancing potential and executes it. Then it performs the misspecification test in Equation (10) to check if the estimated regret coefficient for base learner i_t is consistent with the observed data. If the test triggers, i.e., the $\hat{d}_t^{i_t}$ is too small, then the algorithm doubles it. Lastly, D³RB sets the balancing potential ϕ_t^i to $\hat{d}_t^{i_t} \sqrt{n_t^{i_t}}$.

$$\frac{\hat{u}_t^{i_t}}{n_t^{i_t}} + \frac{\hat{d}_{t-1}^{i_t} \sqrt{n_t^{i_t}}}{n_t^{i_t}} + c \sqrt{\frac{\ln \frac{K \ln n_t^{i_t}}{\delta}}{n_t^{i_t}}} < \max_{j \in [K]} \frac{\hat{u}_t^j}{n_t^j} - c \sqrt{\frac{\ln \frac{K \ln n_t^j}{\delta}}{n_t^j}} \quad (10)$$

Algorithm 2 ORSO with D³RB

Require: MDP $\mathcal{M} = (\mathcal{S}, \mathcal{A}, P, r, \rho_0)$, algorithm \mathfrak{A} , generator G , minimum regret coefficients d_{\min} , failure probability δ

- 1: Sample K reward functions $\mathcal{R}^K = \{f^1, \dots, f^K\} \sim G$
- 2: Initialize K policies $\{\pi^1, \dots, \pi^K\}$
- 3: Initialize balancing potentials $\phi_1^i = d_{\min}$ for all $i \in [K]$
- 4: Initialize regret coefficients $\hat{d}_0^i = d_{\min}$ for all $i \in [K]$
- 5: Initialize counts $n_0^i = 0$ and total values $\hat{u}_0^i = 0$ for all $i \in [K]$
- 6: **for** $t = 1, 2, \dots, T$ **do**
- 7: Select a base learner $i_t \in [K] \in \arg \min_{i \in [K]} \phi_t^i$
- 8: Update $\pi^{i_t} \leftarrow \mathfrak{A}_{f^{i_t}}(\mathcal{M}_{i_t}, N, \pi^{i_t})$
- 9: Evaluate $R_t = \mathcal{J}(\pi^{i_t}) \leftarrow \text{Eval}(\pi^{i_t})$
- 10: // Update necessary variables
- 11: Set $n_t^i = n_{t-1}^i$, $\hat{u}_t^i = \hat{u}_{t-1}^i$, $\hat{d}_t^i = \hat{d}_{t-1}^i$, and $\phi_{t+1}^i = \phi_t^i$ for all $i \in [K] \setminus \{i_t\}$
- 12: Update statistics for current learner $n_t^{i_t} = n_{t-1}^{i_t} + 1$ and $\hat{u}_t^{i_t} = \hat{u}_{t-1}^{i_t} + R_t$
- 13: Perform misspecification test

$$\frac{\hat{u}_t^{i_t}}{n_t^{i_t}} + \frac{\hat{d}_{t-1}^{i_t} \sqrt{n_t^{i_t}}}{n_t^{i_t}} + c \sqrt{\frac{\ln \frac{K \ln n_t^{i_t}}{\delta}}{n_t^{i_t}}} < \max_{j \in [K]} \frac{\hat{u}_t^j}{n_t^j} - c \sqrt{\frac{\ln \frac{K \ln n_t^j}{\delta}}{n_t^j}} \quad (11)$$

- 14: **if** test is triggered **then**
- 15: Double the regret coefficient $\hat{d}_t^{i_t} \leftarrow 2\hat{d}_{t-1}^{i_t}$
- 16: **else**
- 17: Keep the regret coefficient unchanged $\hat{d}_t^{i_t} \leftarrow \hat{d}_{t-1}^{i_t}$
- 18: **end if**
- 19: Update the balancing potential $\phi_{t+1}^{i_t} \leftarrow \hat{d}_t^{i_t} \sqrt{n_t^{i_t}}$
- 20: **end for**
- 21: // Best policy and reward function under the task reward
- 22: **return** $\pi_T^*, f_T^* = \arg \max_{i \in [K]} \mathcal{J}(\pi^i)$

D PROOF OF LEMMA 4.4

In this section, we present the complete proof of Lemma 4.4. We will start by showing that when Assumption 4.2 holds, then with probability at least $1 - \delta$, the estimated regret coefficient of learner i_* will never double provided that $d_{\min} \geq c$, where c is the confidence multiplier in D³RB.

Lemma D.1 (Non-doubling regret coefficient). *When \mathcal{E} holds, and algorithm D³RB is in use*

$$\widehat{d}_t^{i_*} = d_{\min} \quad \text{and} \quad n_T^{i_*} \leq n_T^{i_*} + 1 \quad \text{for all } i \in [K] \quad (12)$$

for all $t \in \mathbb{N}$.

Proof. In order to show this result it is sufficient to show that when \mathcal{E} holds, algorithm i_* does not undergo any doubling event. Doubling of the regret coefficients only happens when the misspecification test triggers for algorithm i_* .

We will show this by induction. Let us assume $\widehat{d}_{t-1}^{i_*} = d_{\min}$ and that $i_t = i_*$. When \mathcal{E} holds, the left-hand side (LHS) of D³RB's misspecification test satisfies

$$\begin{aligned} \frac{\widehat{u}_t^{i_*}}{n_t^{i_*}} + \frac{\widehat{d}_{t-1}^{i_*} \sqrt{n_t^{i_*}}}{n_t^{i_*}} + c \sqrt{\frac{\ln \frac{K \ln n_t^{i_*}}{\delta}}{n_t^{i_*}}} &= \frac{\widehat{u}_t^{i_*}}{n_t^{i_*}} + \frac{\widehat{d}_{t-1}^{i_*} \sqrt{n_t^{i_*}}}{n_t^{i_*}} + c \sqrt{\frac{\ln \frac{K \ln n_t^{i_*}}{\delta}}{n_t^{i_*}}} \quad (i_t = i_*) \\ &\geq \frac{u_t^{i_*}}{n_t^{i_*}} + \frac{\widehat{d}_{t-1}^{i_*} \sqrt{n_t^{i_*}}}{n_t^{i_*}} \quad (\text{event } \mathcal{E}) \\ &\stackrel{(i)}{=} \frac{u_t^{i_*}}{n_t^{i_*}} + \frac{d_{\min} \sqrt{n_t^{i_*}}}{n_t^{i_*}} \quad (13) \end{aligned}$$

where (i) holds because by the induction hypothesis $\widehat{d}_{t-1}^{i_*} = d_{\min}$. We will now show that $n_t^{i_*} \geq n_t^j$ for all $j \in [K]$. Since by the inductive hypothesis $\widehat{d}_\ell^{i_*} = d_{\min}$ for all $\ell \leq t-1$, the potential $\phi_\ell^{i_*} = d_{\min} \sqrt{n_{\ell-1}^{i_*}}$ for all $\ell \leq t$.

For $i \in [K]$ let $t(i)$, be the last time – before time t – algorithm i was played. For $i \neq i_*$ we have $t(i) < t$. Since i was selected at time $t(i)$, by definition of the potentials,

$$\widehat{d}_{t(i)-1}^{i_*} \sqrt{n_{t(i)-1}^{i_*}} = d_{\min} \sqrt{n_{t(i)-1}^{i_*}} \geq \widehat{d}_{t(i)-1}^i \sqrt{n_{t(i)-1}^i} \geq d_{\min} \sqrt{n_{t(i)-1}^i}$$

so that $n_{t(i)-1}^{i_*} \geq n_{t(i)-1}^i$. Since both $n_t^{i_*} = n_{t(i)-1}^{i_*} + 1$ and $n_t^i = n_{t(i)-1}^i + 1$ we conclude that $n_t^{i_*} \geq n_t^i$.

We now turn our attention to the right-hand side (RHS) of D³RB's misspecification test. When \mathcal{E} holds, the RHS of D³RB's misspecification test satisfies,

$$\begin{aligned} \max_{j \in [K]} \frac{\widehat{u}_t^j}{n_t^j} - c \sqrt{\frac{\ln \frac{K \ln n_t^j}{\delta}}{n_t^j}} &\leq \max_{j \in [K]} \frac{u_t^j}{n_t^j} \\ &\stackrel{(i)}{\leq} \max_{j \in [K]} \frac{u_{\binom{i_*}{n_t^j}}}{n_t^j} \\ &\stackrel{(ii)}{\leq} \frac{u_t^{i_*}}{n_t^{i_*}} \quad (14) \end{aligned}$$

where inequalities (i) and (ii) hold because of Assumption 4.2. Combining inequalities 13 and 14 we conclude the misspecification test of algorithm D³RB will not trigger. This finalizes the proof. \square

We are now ready to prove the regret bound on the base learners given in Lemma 4.4.

Lemma 4.4. *Under event \mathcal{E} and Assumption 4.2, with probability $1 - \delta$, the regret of all learners i is bounded in all rounds T as*

$$\sum_{t=1}^{n_T^i} \text{reg}(\pi_{(t)}^i) \leq 6d_T^{i*} \sqrt{n_T^{i*} + 1} + 5c \sqrt{(n_T^{i*} + 1) \ln \frac{K \ln T}{\delta}}, \quad (4)$$

where $d_T^{i*} = d_{(n_T^i)}^{i*}$.

Proof. Consider a fixed base learner i and time horizon T , and let $t \leq T$ be the last round where i was played but the misspecification test did not trigger. If no such round exists, then set $t = 0$. By Corollary 9.1 in Dann et al. (2024), i can be played at most $1 + \log_2 \frac{\bar{d}_T^i}{d_{\min}^i}$ times between t and T , where $\bar{d}_T^i = \max_{\ell \leq T} d_\ell^i$. Thus,

$$\sum_{k=1}^{n_T^i} \text{reg}(\pi_{(k)}^i) \leq \sum_{k=1}^{n_t^i} \text{reg}(\pi_{(k)}^i) + 1 + \log_2 \frac{\bar{d}_T^i}{d_{\min}^i}.$$

If $t = 0$, then the desired statement holds. Thus, it remains to bound the first term in the RHS above when $t > 0$. Since $i = i_t$ and the test did not trigger we have, for any base learner j with $n_t^j > 0$,

$$\begin{aligned} \sum_{k=1}^{n_t^i} \text{reg}(\pi_{(k)}^i) &= n_t^i v^* - u_t^i && \text{(definition of regret)} \\ &= n_t^i v^* - \frac{n_t^i}{n_t^j} u_t^j + \frac{n_t^i}{n_t^j} u_t^j - u_t^i \\ &= \frac{n_t^i}{n_t^j} (n_t^j v^* - u_t^j) + \frac{n_t^i}{n_t^j} u_t^j - u_t^i \\ &= \frac{n_t^i}{n_t^j} \left(\sum_{k=1}^{n_t^j} \text{reg}(\pi_{(k)}^j) \right) + \frac{n_t^i}{n_t^j} u_t^j - u_t^i && \text{(definition of regret)} \\ &\leq \frac{n_t^i}{n_t^j} \left(d_t^j \sqrt{n_t^j} \right) + \frac{n_t^i}{n_t^j} u_t^j - u_t^i && \text{(definition of regret rate)} \\ &= \sqrt{\frac{n_t^i}{n_t^j}} d_t^j \sqrt{n_t^i} + \frac{n_t^i}{n_t^j} u_t^j - u_t^i. \end{aligned}$$

We now focus on $j = i_*$ and use the balancing condition in Lemma 9.2 in Dann et al. (2024) to bound the first factor $\sqrt{n_t^i/n_t^{i*}}$. This condition gives that $\phi_{t+1}^i \leq 3\phi_{t+1}^{i*}$. Since both $n_t^{i*} > 0$ and $n_t^i > 0$, we have $\phi_{t+1}^i = \widehat{d}_t^i \sqrt{n_t^i}$ and $\phi_{t+1}^{i*} = \widehat{d}_t^{i*} \sqrt{n_t^{i*}}$. Thus, we get

$$\sqrt{\frac{n_t^i}{n_t^{i*}}} = \sqrt{\frac{n_t^i}{n_t^{i*}}} \cdot \frac{\widehat{d}_t^i}{\widehat{d}_t^{i*}} \cdot \frac{\widehat{d}_t^{i*}}{\widehat{d}_t^i} = \frac{\phi_{t+1}^i}{\phi_{t+1}^{i*}} \cdot \frac{\widehat{d}_t^{i*}}{\widehat{d}_t^i} \leq 3 \frac{\widehat{d}_t^{i*}}{\widehat{d}_t^i} \leq 3, \quad (15)$$

where the last inequality holds because of Lemma D.1 and because $\widehat{d}_t^i \geq d_{\min}$.

Plugging this back into the expression above and setting $j = i_*$, we have

$$\sum_{k=1}^{n_t^i} \text{reg}(\pi_{(k)}^i) \leq 3d_t^{i*} \sqrt{n_t^i} + \frac{n_t^i}{n_t^{i*}} u_t^{i*} - u_t^i.$$

To bound the last two terms, we use the fact that the misspecification test did not trigger in round t . Therefore,

$$\begin{aligned}
u_t^i &\geq \hat{u}_t^i - c\sqrt{n_t^i \ln \frac{K \ln n_t^i}{\delta}} && \text{(event } \mathcal{E}) \\
&= n_t^i \left(\frac{\hat{u}_t^i}{n_t^i} + c\sqrt{\frac{\ln \frac{K \ln n_t^i}{\delta}}{n_t^i}} + \frac{\hat{d}_t^i \sqrt{n_t^i}}{n_t^i} \right) - 2c\sqrt{n_t^i \ln \frac{K \ln n_t^i}{\delta}} - \hat{d}_t^i \sqrt{n_t^i} \\
&\geq \frac{n_t^i}{n_t^{i*}} \hat{u}_t^{i*} - \sqrt{\frac{n_t^i}{n_t^{i*}}} c\sqrt{n_t^i \ln \frac{K \ln n_t^{i*}}{\delta}} - 2c\sqrt{n_t^i \ln \frac{K \ln n_t^i}{\delta}} - \hat{d}_t^i \sqrt{n_t^i}. && \text{(test not triggered)}
\end{aligned}$$

Rearranging terms and plugging this expression in the bound above gives

$$\begin{aligned}
\sum_{k=1}^{n_t^i} \text{reg}(\pi_{(k)}^i) &\leq 3d_t^{i*} \sqrt{n_t^i} + \sqrt{\frac{n_t^i}{n_t^{i*}}} c\sqrt{n_t^i \ln \frac{K \ln n_t^{i*}}{\delta}} + 2c\sqrt{n_t^i \ln \frac{K \ln n_t^i}{\delta}} + \hat{d}_t^i \sqrt{n_t^i} \\
&\leq 3d_t^{i*} \sqrt{n_t^i} + 3c\sqrt{n_t^i \ln \frac{K \ln n_t^{i*}}{\delta}} + 2c\sqrt{n_t^i \ln \frac{K \ln n_t^i}{\delta}} + \hat{d}_t^i \sqrt{n_t^i} && \text{(Equation (15))} \\
&\leq 3d_t^{i*} \sqrt{n_t^i} + 3c\sqrt{n_t^i \ln \frac{K \ln n_t^{i*}}{\delta}} + 2c\sqrt{n_t^i \ln \frac{K \ln n_t^i}{\delta}} + 3\hat{d}_t^{i*} \sqrt{n_t^i} \\
&&& \text{(Equation (15))} \\
&\leq 3d_t^{i*} \sqrt{n_t^i} + 3\hat{d}_t^{i*} \sqrt{n_t^{i*}} + 5c\sqrt{n_t^i \ln \frac{K \ln t}{\delta}} && (\max(n_t^i, n_t^{i*}) \leq t) \\
&\leq 3d_t^{i*} \sqrt{n_t^i} + 3d_{\min} \sqrt{n_t^{i*}} + 5c\sqrt{n_t^i \ln \frac{K \ln t}{\delta}} && \text{(Lemma D.1)}
\end{aligned}$$

Finally, Lemma D.1 also implies $n_t^i \leq n_t^{i*} + 1$ and since $d_{\min} \leq d_t^{i*}$,

$$\sum_{k=1}^{n_t^i} \text{reg}(\pi_{(k)}^i) \leq 6d_t^{i*} \sqrt{n_t^{i*} + 1} + 5c\sqrt{(n_t^{i*} + 1) \ln \frac{K \ln t}{\delta}}.$$

The statement follows by setting $t = T$. □

E REWARD FUNCTIONS DEFINITIONS

In this section, we present the definition of the human-engineered reward functions and the task reward functions used to evaluate the generated reward in Table 1. The task reward functions are the same as the ones used in Ma et al. (2024).

Table 1: Task reward functions definitions.

ENVIRONMENT	TASK REWARD
CARTPOLE	$\sum \mathbb{1}\{\text{agent is alive}\}$
BALLBALANCE	$\sum \mathbb{1}\{\text{agent is alive}\}$
ANT	$\text{current_distance} - \text{previous_distance}$
HUMNAOID	$\text{current_distance} - \text{previous_distance}$
ALLEGROHAND	$\sum \mathbb{1}\{\text{rotation_distance} < 0.1\}$
SHADOWHAND	$\sum \mathbb{1}\{\text{rotation_distance} < 0.1\}$

The human-designed reward functions from (Makoviychuk et al., 2021) are

- CARTPOLE

$$r = (1.0 - \text{pole_angle}^2 - 0.01 \cdot |\text{cart_vel}| - 0.005 \cdot |\text{pole_vel}|).$$

The reward is additionally multiplied by -2.0 if $|\text{cart_pos}| > \text{reset_dist}$ and multiplied by -2.0 once again if $\text{pole_angle} > \frac{\pi}{2}$.

- BALLBALANCE

$$r = \text{pos_reward} \times \text{speed_reward} = \frac{1}{1 + \text{ball_dist}} \times \frac{1}{1 + \text{ball_speed}},$$

where

$$\text{ball_dist} = \sqrt{\text{ball_pos_x}^2 + \text{ball_pos_y}^2 + (\text{ball_pos_z} - 0.7)^2},$$

where 0.7 is the desired height above the ground, and

$$\text{ball_speed} = \|\text{ball_velocity}\|_2.$$

- ANT and HUMNAOID

$$\begin{aligned} r = & r_{\text{progress}} + r_{\text{alive}} \times \mathbb{1}\{\text{torso_height} \geq \text{termination_height}\} + r_{\text{upright}} \\ & + r_{\text{heading}} + r_{\text{effort}} + r_{\text{act}} + r_{\text{dof}} \\ & + r_{\text{death}} \times \mathbb{1}\{\text{torso_height} \leq \text{termination_height}\}, \end{aligned}$$

where

$$r_{\text{progress}} = \text{current_potential} - \text{previous_potential}$$

$$r_{\text{upright}} = \langle \text{torso_up_vector}, \text{up_vector} \rangle > 0.93$$

$$r_{\text{heading}} = \text{heading_vector} \times \begin{cases} 1.0, & \text{if } \text{norm_angle_to_target} \geq 0.8 \\ \frac{\text{norm_angle_to_target}}{0.8}, & \text{otherwise} \end{cases}$$

$$r_{\text{act}} = -\sum \|\text{actions}\|^2$$

$$r_{\text{effort}} = \sum_{i=1}^N \text{actions}_i \times \text{normalized_motor_strength}_i \times \text{dof_velocity}_i$$

$$\text{potential} = -\frac{\|p_{\text{target}} - p_{\text{torso}}\|_2}{dt}$$

- ALLEGROHAND and SHADOWHAND

$$r = -10r_{\text{dist}} + r_{\text{rot}} - 2 \times 10^{-4}r_{\text{act}}$$

where

$$r_{\text{dist}} = \|p_{\text{obj}} - p_{\text{target}}\|_2$$

$$r_{\text{rot}} = \frac{1}{|\text{rot_dist}| + 0.1}$$

$$r_{\text{act}} = \sum \|\text{actions}\|^2$$

$$\text{rot_dist} = 2 \times \arcsin(\max(1, \|q_{\text{obj}}, \overline{q_{\text{target}}}\|_2))$$

where q is the quaternion and \bar{q} is its conjugate.

F IMPLEMENTATION DETAILS

Rejection Sampling While the LLM produces seemingly good code, this does not guarantee that the sampled code is bug-free and runnable. In ORSO, we employ a simple rejection sampling technique to construct sets of only valid reward functions with high probability, such that reward functions that cannot be compiled or produce $\pm\infty$ or NaN values are discarded.

Given criteria ϕ to be satisfied, our rejection sampling scheme repeats the steps in Algorithm 3 until we have sampled the desired number, K , of valid reward functions.

Algorithm 3 Rejection Sampling in ORSO

```

1: Sample a candidate reward function  $f \sim G$ 
2: if  $\phi(f)$  is satisfied then
3:   Add  $f$  to the set of candidate reward functions
4: else
5:   Reject reward function  $f$ 
6: end if

```

In our practical implementation, checking if criteria ϕ are satisfied consists of instantiating an environment with the generated reward function, running a random policy on it, and checking the values produced by the reward function. If the environment cannot be instantiated or if the values returned by the reward function are $\pm\infty$ or NaN, the reward function is rejected. It is worth making two important observations. First, this is much computationally cheaper than instantiating the environment for training because one does not need to initialize large neural networks and can use fewer parallel environments than the number necessary for training. Moreover, we note that the rejection sampling mechanism only guarantees a higher probability of a valid reward function code as the policy used to evaluate the function is random and the optimization process used during the training of an RL algorithm could still induce undesirable values.

Iterative Improvement of the Reward Function Set In the initial phase of ORSO, the algorithm generates a set of candidate reward functions \mathcal{R}^K for the online reward selection and policy optimization step. While this approach is effective if \mathcal{R}^K contains an effective reward function, any selection process will fail to achieve a high task reward if the set does not contain a good reward function. To address this limitation, we introduce a mechanism for improving the reward function set through iterative resampling and in-context evolution. This is similar to Ma et al. (2024), however, we introduce some important changes to prevent the in-context evolution from overfitting to initially suboptimal reward functions.

Resampling is triggered when at least one reward function has been used to train a policy for the number of iterations specified in the environment configuration or if all the reward functions in the set incurred too large a regret compared to the previous best policy if the algorithm has undergone at least one resampling step.

There are several strategies for resampling reward functions, each with its trade-offs. The simplest approach is to sample new reward functions from scratch, using the same generator G that was used in the initial phase. However, this method may not provide significant improvement, as it essentially restarts the search process without leveraging the information gained from the previous iterations of training.

A more sophisticated approach is to greedily in-context evolve the reward function from the best-performing candidate so far as is done in Ma et al. (2024). This involves making incremental adjustments to the reward function that has shown the most promise, potentially moving it closer to an optimal reward function. However, while this greedy strategy can lead to improvements, it also has the risk of overfitting to an initially suboptimal reward function if, for example, the initial set does not contain effective reward functions.

To mitigate the risk of overfitting, we introduce a simple strategy that allows the algorithm to be more exploratory. Specifically, we combine greedy evolution with random sampling: half of the reward functions are evolved in context from the best-performing candidate, while the other half is sampled from scratch. This approach allows the algorithm to explore new regions of the reward

function space while still exploiting the knowledge gained from previous iterations. We provide the full pseudo-code for ORSO with rejection sampling and iterative improvement in Algorithm 4.

Algorithm 4 ORSO with Rejection Sampling and Iterative Improvement

Require: MDP $\mathcal{M} = (\mathcal{S}, \mathcal{A}, P, r, \rho_0)$, algorithm \mathfrak{A} , generator G , budget T , threshold `n_iters`

- 1: Sample K valid reward functions $\mathcal{R}^K = \{f^1, \dots, f^K\} \sim G$ using Algorithm 3
 - 2: Initialize K policies $\{\pi^1, \dots, \pi^K\}$
 - 3: Initialize selection counts $N^K = \{0, \dots, 0\}$
 - 4: Set $t \leftarrow 1$
 - 5: **while** $t \leq T$ **do**
 - 6: Select a model $i_t \in [K]$ according to a selection strategy
 - 7: Update $\pi^{i_t} \leftarrow \mathfrak{A}_{f^{i_t}}(\mathcal{M}, N, \pi^{i_t})$
 - 8: Evaluate $\mathcal{J}(\pi^{i_t}) \leftarrow \text{Eval}(\pi^{i_t})$
 - 9: Update selection counts: $N^{i_t} \leftarrow N^{i_t} + 1$
 - 10: Update variables (e.g., reward estimates and confidence intervals)
 - 11: **if** $N^{i_t} \geq \text{n_iters}$ or regret w.r.t. previous best is too high **then**
 - 12: Resample $\mathcal{R}^K \sim G$ (half in-context evolution, half from scratch)
 - 13: Sample a new set of reward functions $\mathcal{R}^K = \{f^1, \dots, f^K\}$ using rejection sampling
 - 14: Reset policies $\{\pi^1, \dots, \pi^K\}$
 - 15: Reset selection counts $N^K = \{0, \dots, 0\}$
 - 16: **end if**
 - 17: $t \leftarrow t + 1$
 - 18: **end while**
 - 19: **return** $\pi_T^*, f_T^* = \arg \max_{i \in [K]} \mathcal{J}(\pi^i)$
-

G SELECTION ALGORITHMS AND HYPERPARAMETERS

In this section, we present the pseudocode for all reward selection algorithms used in our experiments with their associated hyperparameters in Table 2.

Algorithm 5 ε -Greedy

Require: Number of arms K , total time T , exploration probability ε

- 1: Initialize counts $n_0^i = 0$ and total values $\hat{u}_0^i = 0$ for all $i \in [K]$
- 2: **for** $t = 1, \dots, T$ **do**
- 3: Select arm

$$i_t = \begin{cases} \arg \max_i (\hat{u}_t^i / n_t^i), & \text{with probability } 1 - \varepsilon \\ i \sim \text{Uniform}([K]), & \text{with probability } \varepsilon \end{cases}$$

- 4: Play arm i_t and observe reward r_t
 - 5: Set $n_t^i = n_{t-1}^i$, and $\hat{u}_t^i = \hat{u}_{t-1}^i$ for all $i \in [K] \setminus \{i_t\}$
 - 6: Update statistics for current learner $n_t^{i_t} = n_{t-1}^{i_t} + 1$ and $\hat{u}_t^{i_t} = \hat{u}_{t-1}^{i_t} + r_t$
 - 7: **end for**
-

Algorithm 6 Explore-then-Commit

Require: Number of arms K , total time T , exploration phase length T_0

- 1: Initialize counts $n_0^i = 0$ and total values $\hat{u}_0^i = 0$ for all $i \in [K]$
 - 2: *// Explore*
 - 3: **for** $t = 1, \dots, T_0$ **do**
 - 4: Select arm $i_t = (t \bmod K) + 1$
 - 5: Play arm i_t and observe reward r_t
 - 6: Set $n_t^i = n_{t-1}^i$, and $\hat{u}_t^i = \hat{u}_{t-1}^i$ for all $i \in [K] \setminus \{i_t\}$
 - 7: Update statistics for current learner $n_t^{i_t} = n_{t-1}^{i_t} + 1$ and $\hat{u}_t^{i_t} = \hat{u}_{t-1}^{i_t} + r_t$
 - 8: **end for**
 - 9: *// Commit*
 - 10: $i_\star = \arg \max_i (\hat{u}_{T_0}^i / n_{T_0}^i)$
 - 11: **for** $t = T_0 + 1$ to T **do**
 - 12: Play arm i_\star and observe reward r_t
 - 13: **end for**
-

Algorithm 7 UCB (Upper Confidence Bound)

Require: Number of arms K , total time T , confidence multiplier c

- 1: Initialize counts $n_0^i = 0$ and total values $\hat{u}_0^i = 0$ for all $i \in [K]$
- 2: **for** $t = 1, \dots, K$ **do**
- 3: Select arm $i_t = t$
- 4: Play arm i_t and observe reward r_t
- 5: Update statistics for current learner $n_t^{i_t} = n_{t-1}^{i_t} + 1$ and $\hat{u}_t^{i_t} = \hat{u}_{t-1}^{i_t} + r_t$
- 6: **end for**
- 7: **for** $t = K + 1, \dots, T$ **do**
- 8: Select arm

$$i_t = \arg \max_i \left(\frac{\hat{u}_t^i}{n_t^i} + c \sqrt{2 \frac{\ln t}{n_t^i}} \right)$$

- 9: Play arm i_t and observe reward r_t
 - 10: Set $n_t^i = n_{t-1}^i$, and $\hat{u}_t^i = \hat{u}_{t-1}^i$ for all $i \in [K] \setminus \{i_t\}$
 - 11: Update statistics for current learner $n_t^{i_t} = n_{t-1}^{i_t} + 1$ and $\hat{u}_t^{i_t} = \hat{u}_{t-1}^{i_t} + r_t$
 - 12: **end for**
-

Algorithm 8 Exp3 (Exponential-weight algorithm for Exploration and Exploitation)**Require:** Number of arms K , total time T , learning rate η

- 1: Initialize weights $w_0^i = 1$ and probabilities $p_0^i = 1/K$ for all $i \in [K]$
- 2: **for** $t = 1, \dots, T$ **do**
- 3: Select arm i_t according to distribution $P_t = [p_t^1, \dots, p_t^K]$
- 4: Play arm i_t and observe reward r_t
- 5: Estimate reward $\hat{r}_t = r_t/p_t^{i_t}$
- 6: Update weight $w_t^{i_t} = w_{t-1}^{i_t} \exp(\eta \hat{r}_t/K)$
- 7: Update probabilities

$$p_t^i = (1 - \eta) \frac{w_t^i}{\sum_{j=1}^K w_t^j} + \frac{\eta}{K} \quad \text{for all } i \in [K]$$

8: **end for**

Table 2: Hyperparameters for MAB Algorithms

ALGORITHM	PARAMETER	VALUE
EPSILON-GREEDY	ε	0.1
EXPLORE-THEN-COMMIT	T_0	$5 \cdot K$
UCB	c	1.0
EXP3	η	0.1

H ADDITIONAL EXPERIMENTAL RESULTS

In this section, we report additional experimental evaluations. In particular, we show how different configurations of budget constraints B and sizes K of the reward function set perform with different reward selection algorithms in different environments in Figures 6 to 9.

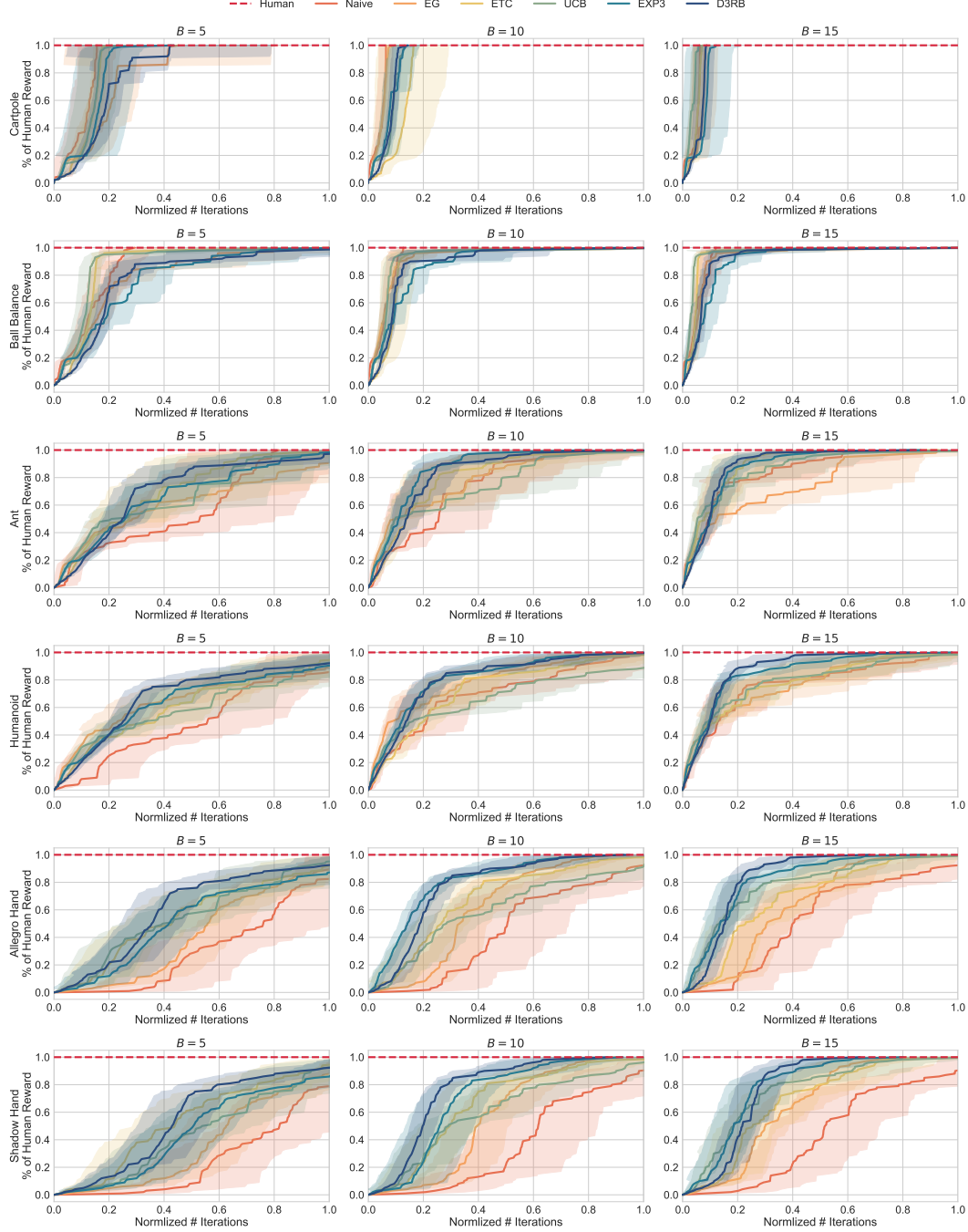


Figure 6: Number of iterations necessary to reach human-engineered reward function performance with different computation budgets and tasks. The shaded areas represent 95% confidence intervals. To construct this plot, we sample the first index when the performance reaches each percentage point from 1% to 100% of human performance during training.

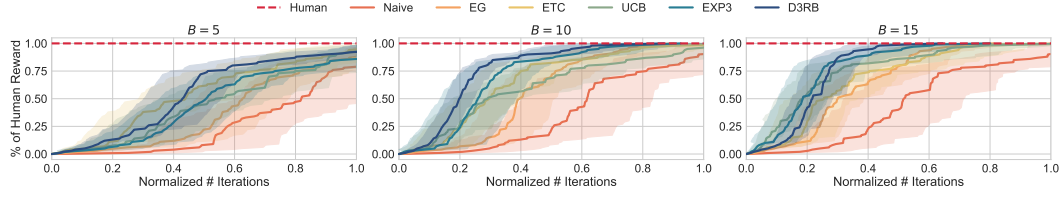


Figure 7: Number of iterations necessary to reach human-engineered reward function performance with different computation budgets. The shaded areas represent 95% confidence intervals.

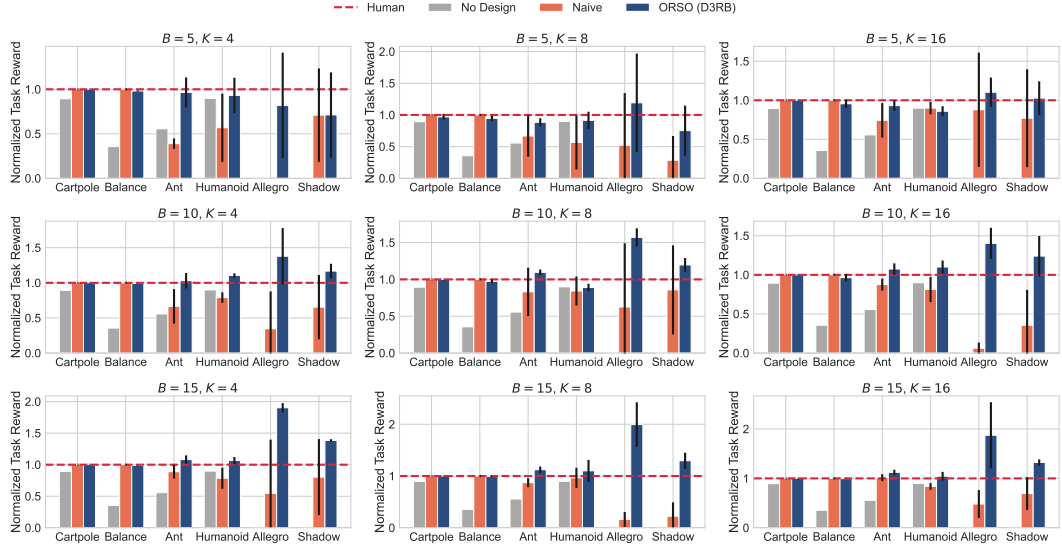


Figure 8: Average performance with 95% confidence intervals for ORSO with different budget constraints and reward function set size. The red horizontal dashed line represents the policies trained with the human-engineered reward function.

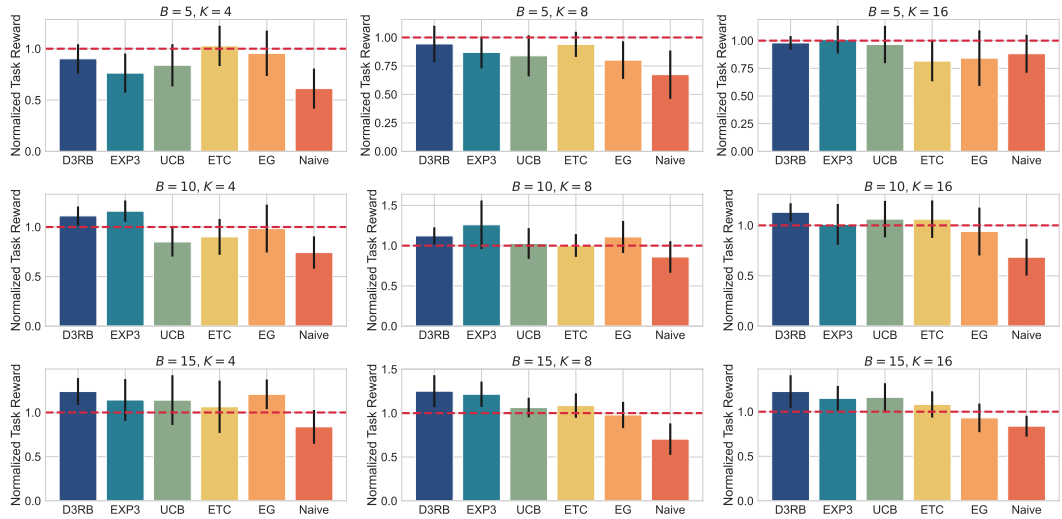


Figure 9: Comparison of different reward selection algorithms for ORSO with different budget constraints and reward function set size.

H.1 VISUALIZING ORSO

To better visualize how ORSO selects the best reward function, discards suboptimal ones efficiently, and thanks to this, explores more reward functions, we provide further visualizations in this section.⁵

Figures 10 and 11 show a full training of ORSO (D³RB) and EUREKA with a budget $B = 15$ and $K = 16$ on the ALLEGROHAND task, respectively. In both figures, the top plot shows the task reward during training. The colors indicate the reward functions currently in use. The middle plot more clearly shows the reward function being currently used. The vertical axis contains the reward function indices. In both plots, the dashed vertical lines indicate that a resampling has been triggered. Lastly, the bottom plot shows the unnormalized cumulative regret during training.

Comparing the two figures, we can see that ORSO initially explores all reward functions near-uniformly, but quickly finds a policy that surpasses the policy from the human-engineered reward function, leading to a decrease in regret. On the other hand, EUREKA uniformly trains on each reward function leading the algorithm to explore fewer reward functions. Moreover, we see that the lack of rejection sampling can result in initial reward function sets that contain many invalid reward functions – indicated by a \times in the figures.

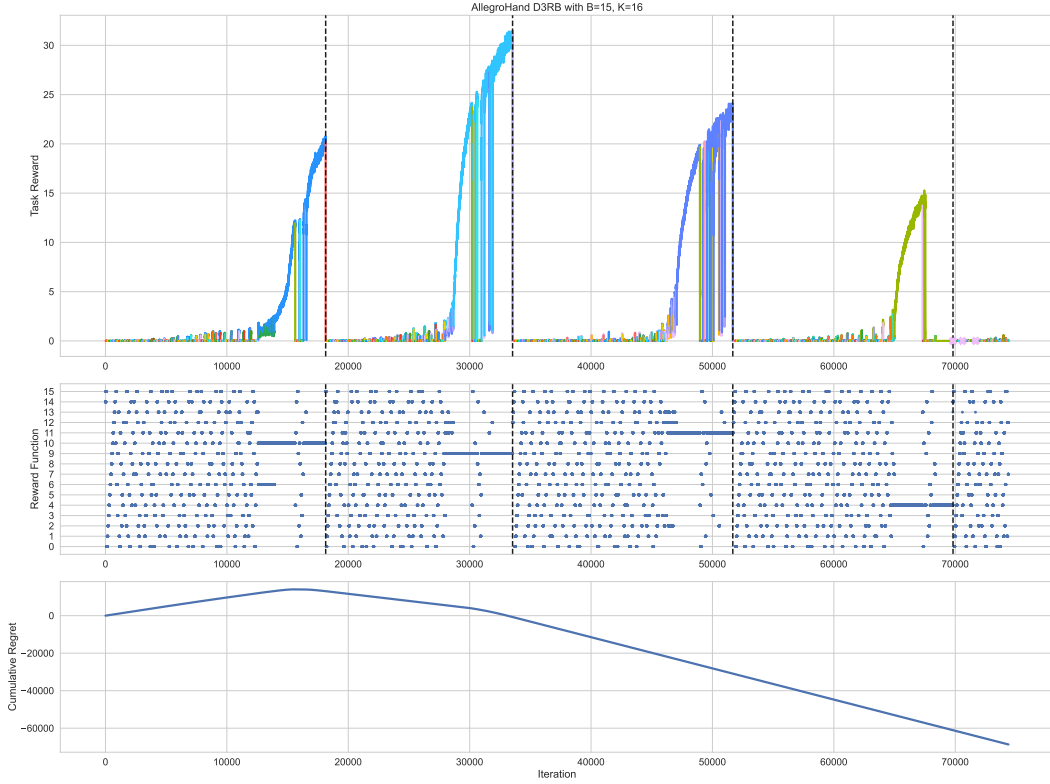
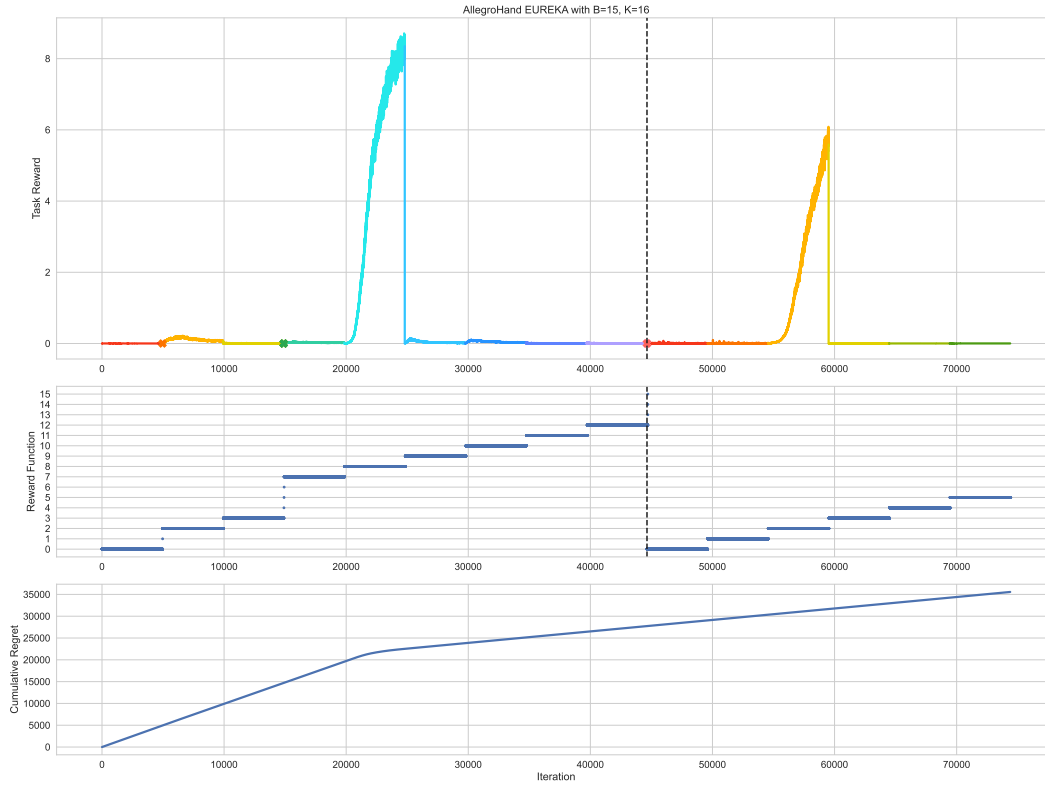
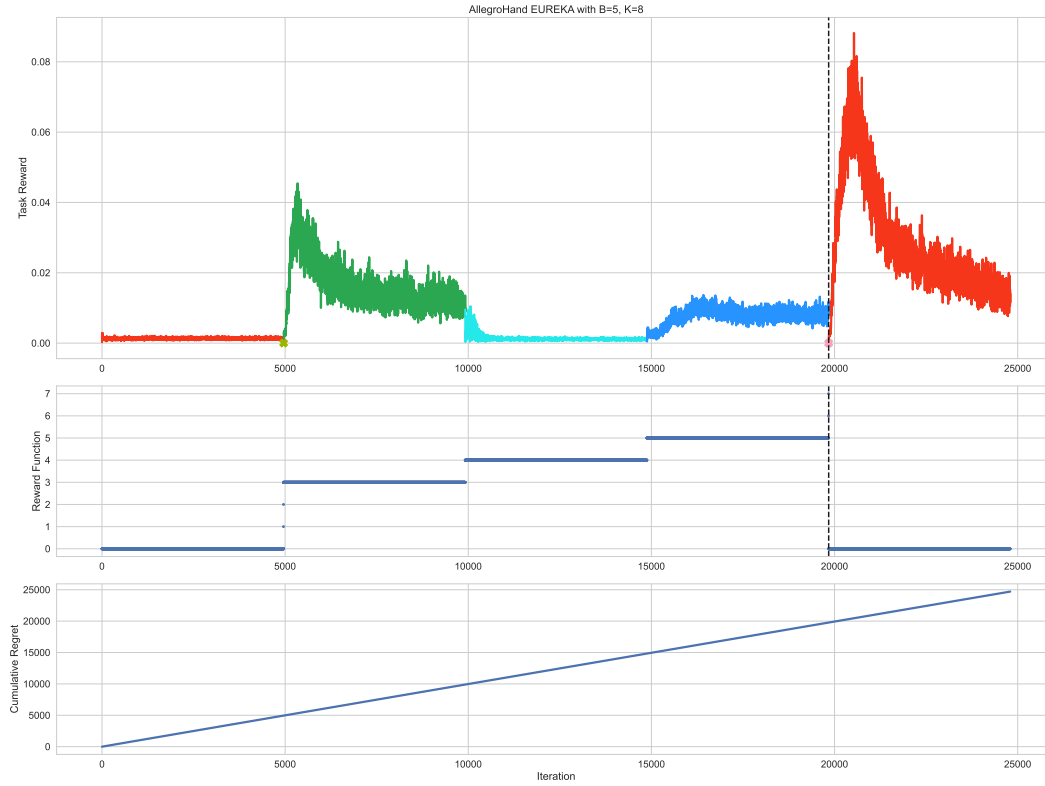


Figure 10: ORSO (D³RB) on ALLEGROHAND with $B = 15$ and $K = 16$.

⁵Additional animated visualizations can also be found at <https://calvincbzhong.github.io/orso-website/>.

Figure 11: EUREKA on ALLEGROHAND with $B = 15$ and $K = 16$.Figure 12: EUREKA on ALLEGROHAND with $B = 5$ and $K = 8$.

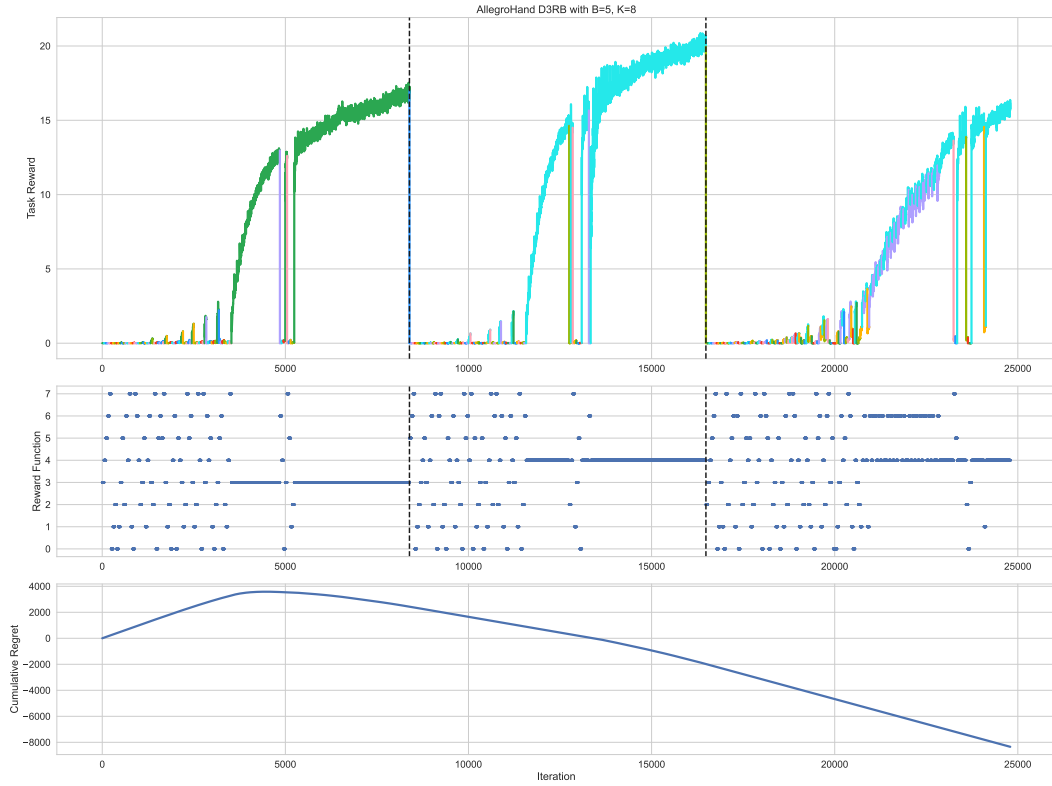


Figure 13: ORSO (D^3RB) on ALLEGROHAND with $B = 5$ and $K = 8$.

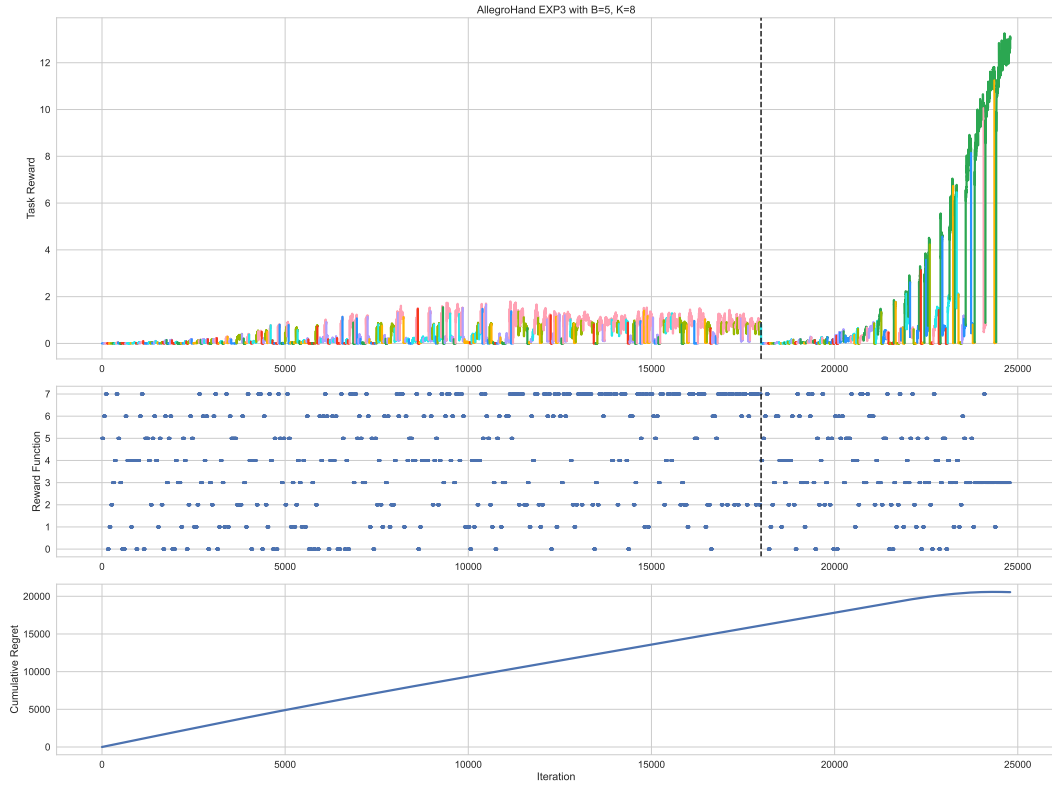
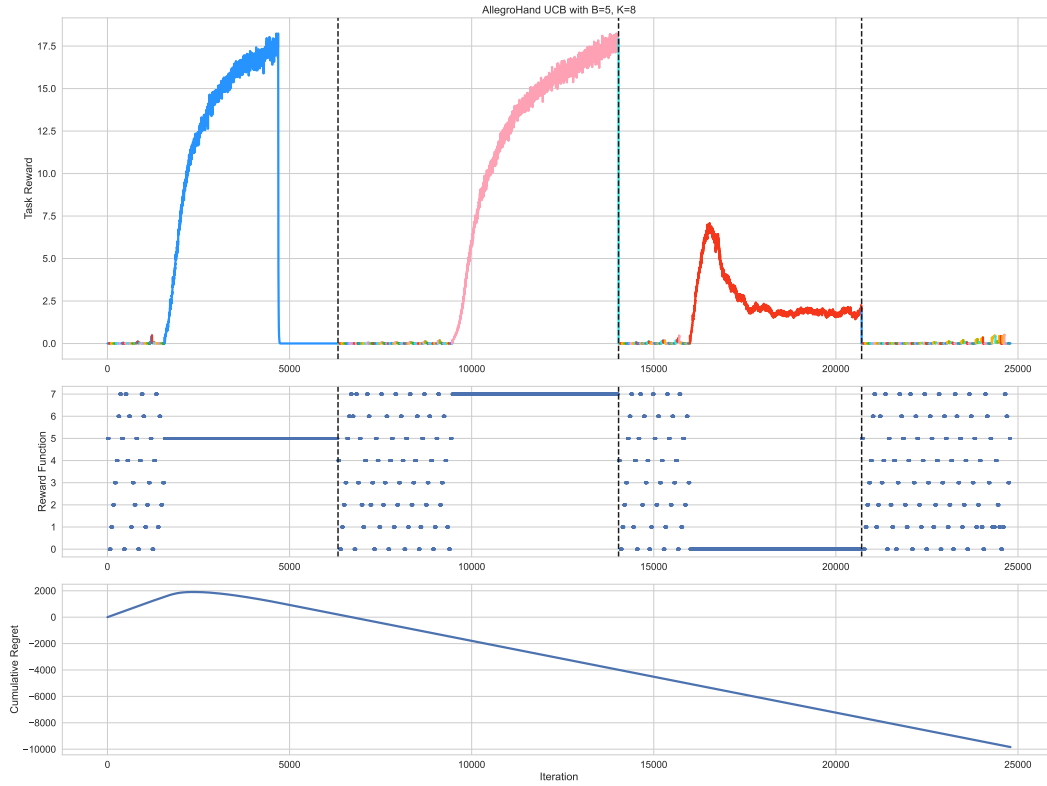
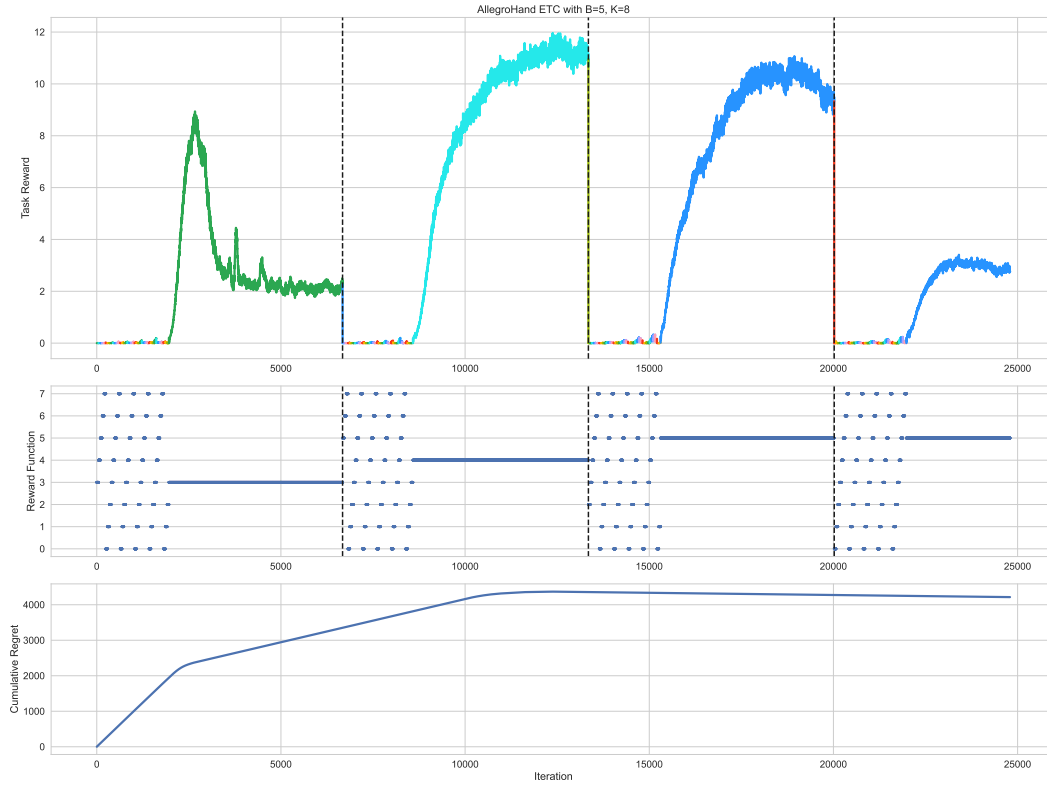


Figure 14: ORSO (Exp3) on ALLEGROHAND with $B = 5$ and $K = 8$.

Figure 15: ORSO (UCB) on ALLEGROHAND with $B = 5$ and $K = 8$.Figure 16: ORSO (ETC) on ALLEGROHAND with $B = 5$ and $K = 8$.

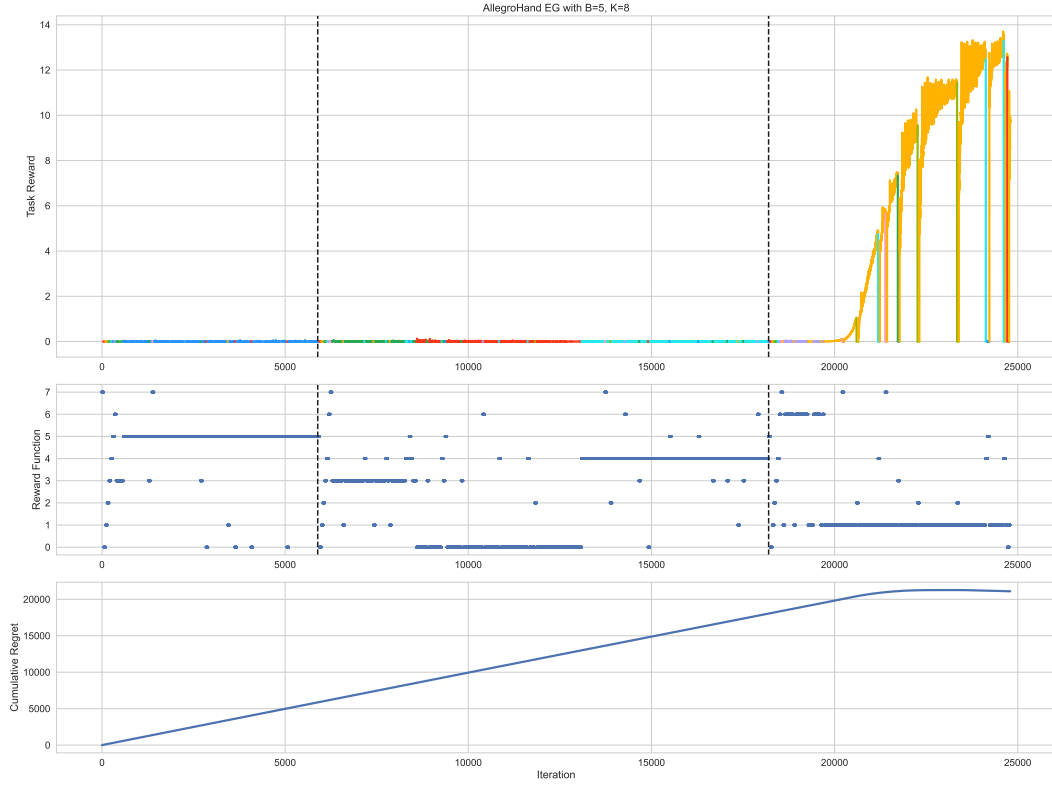


Figure 17: ORSO (EG) on ALLEGROHAND with $B = 5$ and $K = 8$.

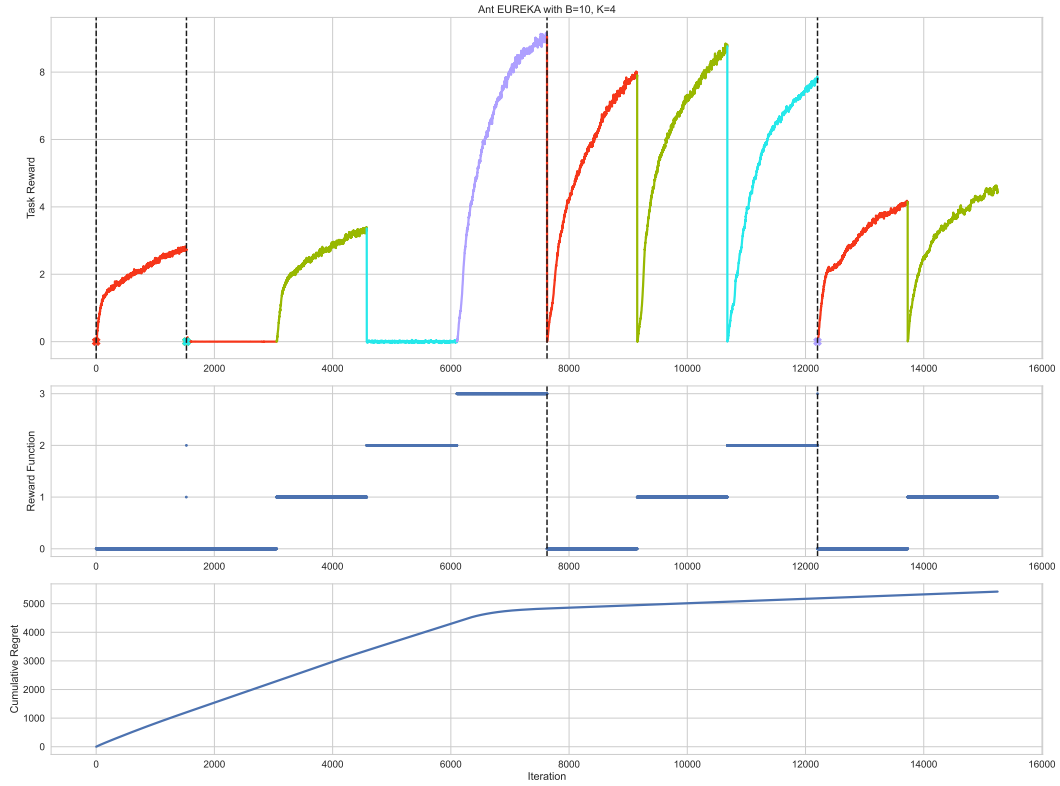
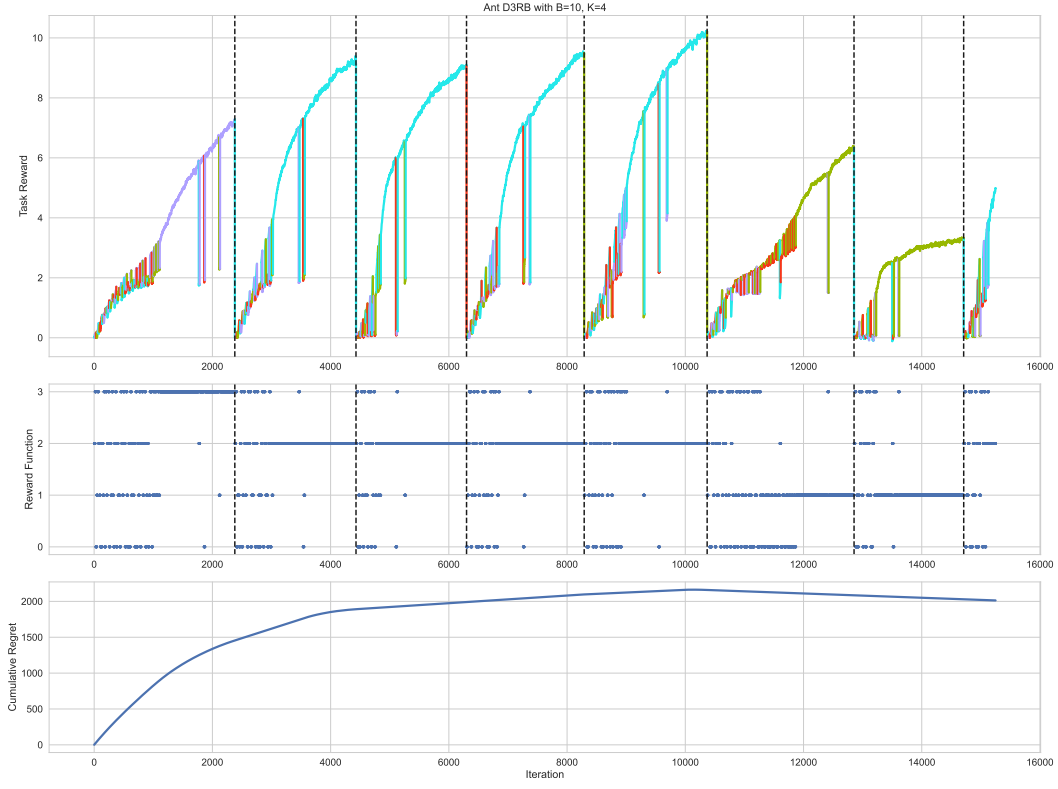
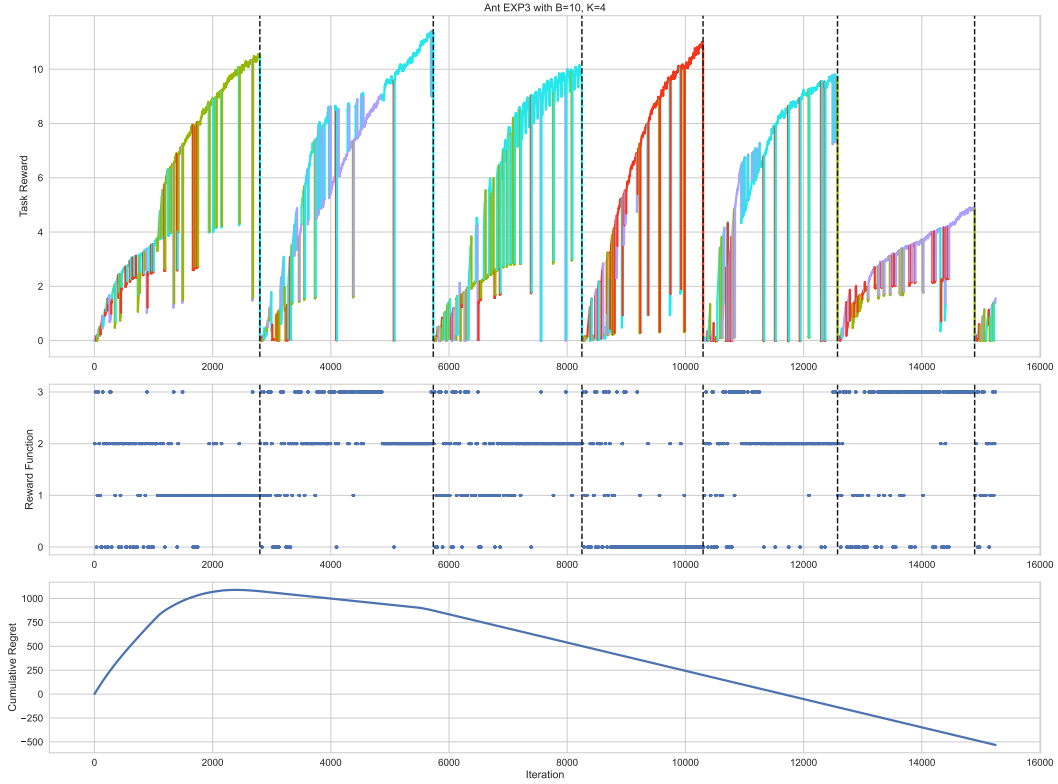
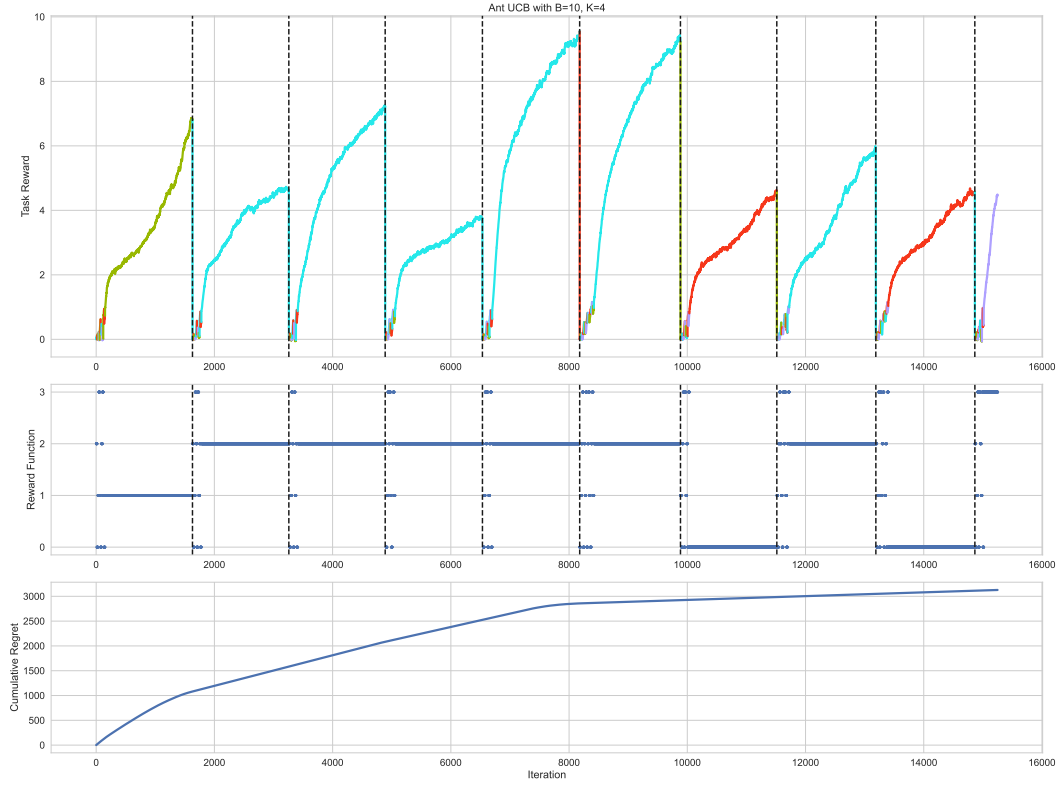
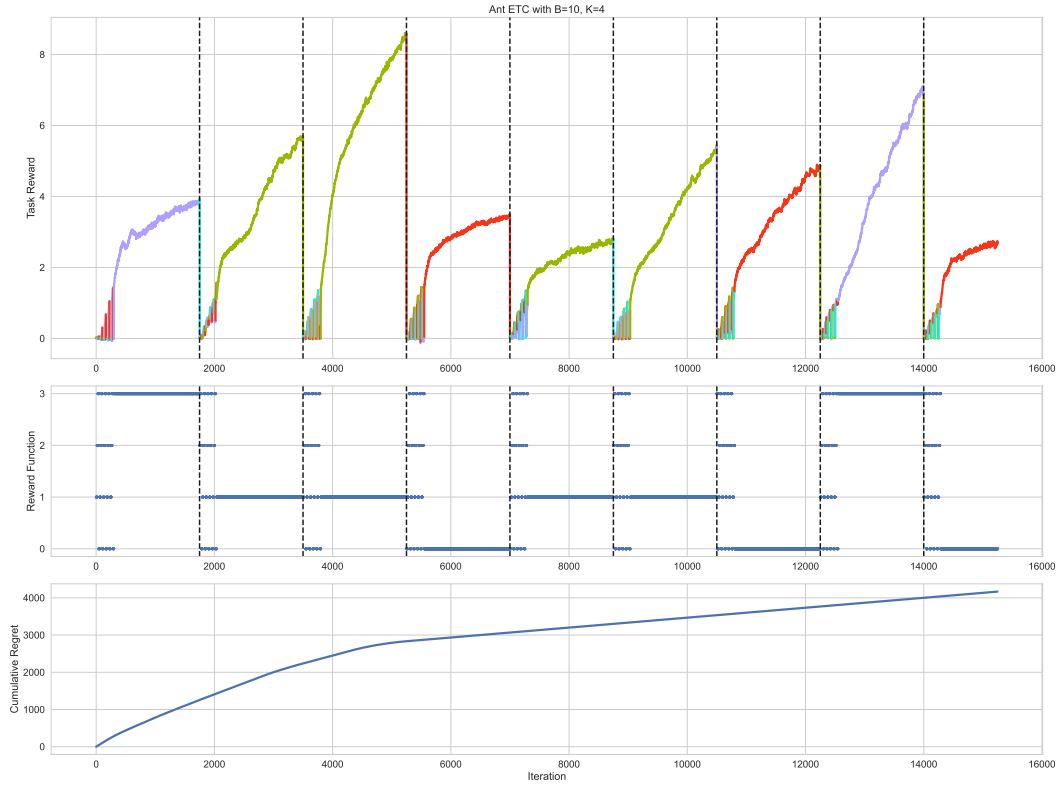


Figure 18: EUREKA on ANT with $B = 10$ and $K = 4$.

Figure 19: ORSO (D³RB) on ANT with $B = 10$ and $K = 4$.Figure 20: ORSO (Exp3) on ANT with $B = 10$ and $K = 4$.

Figure 21: ORSO (UCB) on ANT with $B = 10$ and $K = 4$.Figure 22: ORSO (ETC) on ANT with $B = 10$ and $K = 4$.

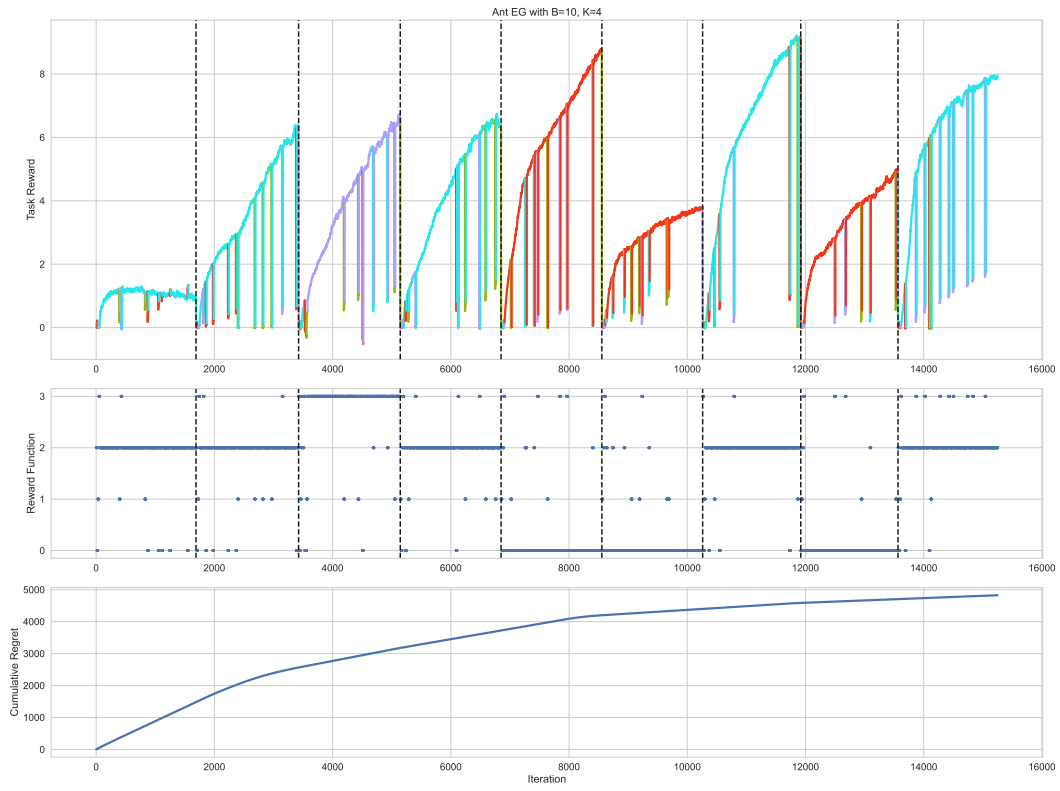


Figure 23: ORSO (EG) on ANT with $B = 10$ and $K = 4$.